

BIOTRANSFORMATION OF ACETAMINOPHEN BY FOUR PHYLOGENETICALLY
DISTINCT BACTERIA AND IMMOBILIZED ENZYMES OF *RHODOCOCCUS*
ERYTROPOLIS BIOMIG-P19

by

Çağlar Akay

BS. in E.Eng., Yildiz Technical University, 2014

Submitted to the Institute of Environmental Sciences in partial fulfillment of
the requirements for the degree of
Master of Science
in
Environmental Technology

Boğaziçi University

2017

ACKNOWLEDGEMENTS

I would first like to express my sincere gratitude to my graduate advisor Asst. Prof. Dr. Ulaş Tezel for the continuous support he has provided during my study and research, for his patience, encouragement, motivation and extensive knowledge. The door of his office was always open whenever I needed. I could not have imagined having a better mentor. I also extend my appreciation to the members of my thesis committee: Prof. Dr. Nilsun İnce and Assoc. Prof. Dr. Elif Pehlivanoğlu Mantaş for allocating their time to evaluate my study.

My sincere thanks also goes to my fellow lab mates Emine Ertekin, Gökçin Gül, Koray Sakarya, Seyedmehdi Emadian, Özgücan Eken and Begüm Şepitci for their wonderful collaboration, for their willingness to help any time needed, and for all the fun we have had together. With a special mention to Elif Irmak Erdem, Gülşah Günel, Cansu Çetin, Ayşe Mergenci, Öncü Maracı, İbrahim Halil Miraloğlu, and İlknur Temizel. It was fantastic to have such great colleagues!

I am also grateful to my friends for their sympathetic ear and their support along the way. Love you all guys!

And finally, I must express my profound gratitude to my mom and my brother for providing me with unfailing support and motivation throughout my life in general. Thank you!

This research was supported by The Scientific and Technological Research Council of Turkey (TUBITAK, 113Y528).

**BIOTRANSFORMATION OF ACETAMINOPHEN BY FOUR
PHYLOGENETICALLY DISTINCT BACTERIA AND
IMMOBILIZED ENZYMES OF *RHODOCOCCUS ERYTHROPOLIS*
BIOMIG-P19**

Acetaminophen (APAP) is the active ingredient of commonly used antipyretic and analgesic drugs; therefore it is one of the most frequently detected emerging micropollutant in the environment. In this study, four bacterial species capable of degrading APAP were isolated from soil microbial community developed by selective enrichment. Predominant APAP degrader in the community was a strain of *Rhodococcus erythropolis*. Other APAP degraders included strains of *Pseudomonas nitroreducens*, *Flavobacterium* sp., and *Sphingobium* sp. Among them the strains of *Flavobacterium* sp. and *Sphingobium* sp. are novel APAP-degraders, which have not been reported in the literature to date. A series of kinetic experiments in shake-flasks with *Rhodococcus erythropolis* BIOMIG-P19 were performed to evaluate the effect of APAP concentration, cell density and temperature on APAP biotransformation and to elucidate the APAP biotransformation pathway. The maximum cell specific APAP utilization rate and half-saturation APAP concentration constants were calculated as $133 \pm 7 \times 10^{-11}$ mg/cell.hr and 211 ± 28 mg/L, respectively. Optimum APAP biotransformation temperature was calculated as 28°C. *p*-aminophenol was identified as the major biotransformation by-product using tandem mass spectroscopy. Complete utilization of APAP by immobilized enzymes of BIOMIG-P19 at 1.5 mg protein and 10 mg/L APAP concentration lasted 12 days.

**ACETAMİNOFEN'İN FİLOGENETİK OLARAK BİRBİRİNDEN
FARKLI 4 BAKTERİ TÜRÜ VE İMMOBİLİZE EDİLMİŞ
RHODOCOCCUS ERYTHROPOLIS BIOMIG-P19 CİNSİ BAKTERİ
ENZİMLERİ TARAFINDAN BİYODÖNÜŞÜMÜ**

Acetaminofen (APAP) yaygın olarak kullanılmakta olan antipiretik ve analjezik bir ilaç hammaddesidir. Buna bağlı olarak doğada en sık karşılaşılan mikrokirleticiler arasında sayılmaktadır. Bu çalışmada, APAP'ı 50 mg/L konsantrasyonda parçalama özelliğine sahip 4 farklı bakteri cinsi, toprak numunesi ile zenginleştirilmiş mikrobiyal topluluktan izole edilmiştir. Bu bakteri topluluğunda APAP'ı parçalayan baskın tür *Rhodococcus erythropolis*; diğer izolatlar ise *Pseudomonas nitroreducens*, *Flavobacterium* sp., ve *Sphingobium* sp. türleri olarak belirlenmiştir. Bu türler arasında literatürde daha önce rapor edilmemiş olan *Flavobacterium* sp. ve *Sphingobium* sp.'in ise yeni türler olduğu görülmüştür. APAP konsantrasyonu, bakteri yoğunluğu ve sıcaklığın etkileri ile APAP biyodönüşüm yolizini tayin etmek amacıyla *Rhodococcus erythropolis* BIOMIG-P19 türü ile bir dizi kinetik deneyi gerçekleştirilmiştir. Maksimum hücresel APAP parçalama hız ve yarı doygunluk sabitleri sırasıyla $133 \pm 7 \times 10^{-11}$ mg/hücre.sa ve 211 ± 28 mg/L olarak belirlenmiştir. Optimum APAP biyotransformasyon sıcaklığı 28°'dir. Biyotransformasyonun en önemli yan ürünü, tandem kütle spektroskopisi kullanılarak *p*-aminofenol olarak belirlenmiştir. BIOMIG-P19'dan ekstrakte edilerek immobilize edilmiş enzimler ile APAP'ın tamamen parçalanması 1.5 mg protein ve 10 mg/L APAP konsantrasyonunda 12 gün sürmüştür.

TABLE OF CONTENTS

| | |
|--|------|
| ACKNOWLEDGEMENTS | iii |
| ABSTRACT | iv |
| ÖZET | v |
| LIST OF FIGURES | viii |
| LIST OF TABLES | xi |
| LIST OF SYMBOLS/ABBREVIATIONS | xii |
| 1. INTRODUCTION | 1 |
| 2. LITERATURE SURVEY | 5 |
| 2.1. APAP in General | 5 |
| 2.2. Occurrence of APAP in the Environment | 6 |
| 2.3. Ecotoxicity of APAP | 8 |
| 2.4. Biodegradation of APAP | 11 |
| 3. MATERIALS AND METHODS | 15 |
| 3.1. Chemicals | 15 |
| 3.2. Development of APAP Degrading Soil Microbial Community | 15 |
| 3.3. Isolation of APAP Degraders in the Enrichment Community | 15 |
| 3.4. Identification of APAP Degraders Based on 16S rRNA Gene | 16 |
| 3.5. LB Growth Assay | 17 |
| 3.6. Kinetic Assays | 17 |
| 3.7. Oxygen Threshold Concentration for APAP Biotransformation | 18 |
| 3.8. APAP Biotransformation Kinetics using Crude Enzymes of BIOMIG-P Cells | 19 |
| 3.9. Protein Extraction and SDS-PAGE | 20 |
| 3.10. Ca-Alginate Bead Preparation | 22 |
| 3.11. Kinetic Experiments with Enzyme Beads | 23 |
| 3.12. Analytical Methods | 23 |
| 4. RESULTS AND DISCUSSION | 27 |
| 4.1. Activity of APAP Degrading Community | 27 |
| 4.2. Phylogenetic Identification of APAP Degraders Based on 16S rRNA Gene | 28 |
| 4.3. APAP Biotransformation Kinetics of Four Isolates | 29 |
| 4.4. Growth Kinetics of BIOMIG-P19 | 31 |

| | |
|--|----|
| 4.5. APAP Biotransformation by BIOMIG-P19 | 34 |
| 4.5.1. Effect of initial APAP concentration | 34 |
| 4.5.2. Effect of initial cell density | 36 |
| 4.5.3. Effect of temperature | 38 |
| 4.6. Threshold O ₂ Concentration for APAP Biotransformation | 40 |
| 4.7. Determination of APAP Biotransformation Pathway | 40 |
| 4.8. Enzyme Kinetics of BIOMIG-P cells | 44 |
| 4.9. APAP Biotransformation Kinetics of Enzyme Beads | 46 |
| 5. CONCLUSIONS | 49 |
| REFERENCES | 50 |

LIST OF FIGURES

| | |
|---|----|
| Figure 2.1. Molecular structure of Acetaminophen | 5 |
| Figure 2.2. Proposed pathway for APAP biotransformation from the previous studies | 14 |
| Figure 3.1. Closed bottle set-up used for determining APAP biotransformation under limiting O ₂ concentration | 19 |
| Figure 3.2. Schematic representation of SDS-PAGE setup | 22 |
| Figure 3.3. Ca-alginate bead preparation setup | 23 |
| Figure 3.4. Sample HPLC chromatogram of APAP in mobile phase | 24 |
| Figure 3.5. Mass and molar calibration curves of APAP | 24 |
| Figure 3.6. EMS spectra of APAP using DP at 56 V, EP at 10 V and CE at 23 V | 26 |
| Figure 4.1. APAP degrading microbial community development | 27 |
| Figure 4.2. Phylogenetic tree of relationships based on 16S rDNA sequence of BIOMIG-P isolates determined by maximum likelihood followed by UPGMA tree building method and Jukes-Cantor genetic distance model, relative to other bacterial strains | 28 |
| Figure 4.3. APAP utilization profiles by (A) <i>Pseudomonas nitroreducens</i> BIOMIG-P2, (B) <i>Rhodococcus erythropolis</i> BIOMIG-P19, (C) <i>Flavobacterium</i> sp. BIOMIG-P32, and (D) <i>Sphingobium</i> sp. BIOMIG-P36 at 10 mg/L concentration at 22°C (error bars represent one standard deviation of the mean, $n=3$) | 30 |

| | |
|--|----|
| Figure 4.4. Growth profile of BIOMIG-P19 in LB broth at (A) 5°C, (B) 10°C, (C) 15°C, (D) 22°C, (E) 30°C, (F) 35°C, (G) 40°C and (H) 45°C | 32 |
| Figure 4.5. Relationship between temperature and growth rate | 34 |
| Figure 4.6. Profiles of APAP utilization by BIOMIG-P19 at (A) 1 and 10 mg/L and (B) 100 and 500 mg/L concentration at 22°C | 35 |
| Figure 4.7. Cell specific biotransformation rate at APAP concentrations between 1 and 500 mg/L | 36 |
| Figure 4.8. Profiles of APAP utilization by BIOMIG-P19 at 10 mg/L initial APAP concentration and different cell densities between 10^9 and 10^{11} CFU/L at 22°C | 37 |
| Figure 4.9. Profile of APAP biotransformation rates at cell densities between 10^{10} to 10^{11} CFU/L | 37 |
| Figure 4.10. Profiles of APAP utilization by BIOMIG-P19 at (A) CONTROL, (B) 5°C, (C) 10°C, (D) 15°C, (E) 2°C, (F) 3°C, (G) 35°C and (H) 45°C at 10 mg/L | 38 |
| Figure 4.11. Profile of APAP biotransformation rate at 10 mg/L initial APAP concentration between 5 and 45°C | 39 |
| Figure 4.12. Profiles of headspace oxygen and carbon dioxide, spiked with 100 mg/L initial APAP concentration in control and test serum bottles inoculated with BIOMIG-P19 | 39 |
| Figure 4.13. Overlaid EMS spectrum of samples taken at t=0 and t=6 hours showing the major parent compound distribution and change over time | 40 |

- Figure 4.14. EPI spectrum of M1 with the proposed ion fragments. The molecular weight of M1 is 109. The m/z 110 corresponds to the $[M+H]^+$ parent ion 41
- Figure 4.15. EPI spectrum of M2 with the proposed ion fragments. The molecular weight of M2 is 110. The m/z 111 corresponds to the $[M+H]^+$ parent ion 41
- Figure 4.16. EPI spectrum of M3 with the proposed ion fragments. The molecular weight of M3 is 108. The m/z 108 corresponds to the $[M]^+$ parent ion 42
- Figure 4.17. APAP and its biotransformation by-products inoculated with BIOMIG-P19 43
- Figure 4.18. Proposed pathway of APAP biotransformation by BIOMIG-P19 43
- Figure 4.19. SDS-PAGE with protein ladder standard Precision Plus Protein™ Dual Xtra from Bio-Rad. Comparison of crude protein between BIOMIG-P2, BIOMIG-P19, BIOMIG-P32 and BIOMIG-P36. (*: Indicates the cells induced with acetaminophen prior to cell disruption) 44
- Figure 4.20. Profiles of APAP utilization by Enzymes of (A) BIOMIG-P2, (B) BIOMIG-P19, (C) BIOMIG-P32 and (D) BIOMIG-P36 cells at 10 mg/L initial APAP concentration (k: mg APAP/mg protein.hour) 45
- Figure 4.21. Profiles of APAP utilization by immobilized enzymes of BIOMIG-P19 46
- Figure 4.22. Proposed mechanisms initiating APAP biotransformation by immobilized enzymes 47

LIST OF TABLES

| | |
|--|----|
| Table 4.1. Biotransformation rate constants of BIOMIG-P isolates at 10 mg/L initial APAP concentration | 30 |
| Table 4.2. Calculated specific growth rate and doubling time in LB broth at 5, 10, 15, 22, 30, 35 and 45°C | 33 |
| Table 4.3. Biotransformation rate constants at APAP concentrations at 1, 10, 100 and 500 mg/L | 36 |

LIST OF SYMBOLS/ABBREVIATIONS

| Symbol | Explanation | Units used |
|---------------|--|-------------------|
| APAP | Acetaminophen | |
| BCF | Bioconcentration Factor | |
| CE | Collision Energy | |
| CFU | Colony Forming Unit | |
| DI | Deionized Water | |
| DNA | Deoxyribonucleic Acid | |
| DP | Declustering Potential | |
| EMS | Enhanced Mass Spectrum | |
| EP | Entrance Potential | |
| EPI | Enhanced Product Ion | |
| ESI | Electron Spray Ionization | |
| GC | Gas Chromatography | |
| HMDB | Human Metabolome Database | |
| HPLC | High Pressure Liquid Chromatography | |
| HQ | Hazard Quotients | |
| LB | Luria Bertani | |
| MBR | Membrane Bioreactor | |
| MOPS | 3-N-morpholino Propane Sulfonic Acid | |
| MS/MS | Tandem Mass Spectrometer | |
| NAPQI | <i>N</i> -acetyl- <i>p</i> -benzoquinone imine | |
| OR | Orientation | |
| PCR | Polymerase chain reaction | |
| PhACS | Pharmaceutically Active Compounds | |
| R | Functional group | |
| RNA | Ribonucleic Acid | |
| RNS | Reactive Nitrogen Species | |
| ROS | Reactive Oxygen Species | |
| SBR | Sequencing Batch Reactor | |
| SDS | Sodium Dodecyl Sulfonate | |

| Symbol | Explanation | Units used |
|---------------|--|--------------------------------------|
| TEMED | Tetramethylethylenediamine | |
| US EPA | U.S. Environmental Protection Agency | |
| WWTPs | Wastewater treatment plants | |
| μ | Specific growth rate | (hr) |
| t_d | Time required for cells to double itself | (1/hr) |
| OD | Optical density | (nm) |
| $[APAP]$ | APAP concentration | (mg/L) |
| K_{APAP} | Half-saturation constant | (mg/L) |
| X | Cell density | (cells/L) |
| k | Cell specific rate of APAP utilization | (mg/cells.hr) |
| k' | Observed rate of APAP utilization | (mg/L.hr) |
| EC_{50} | Inhibitor concentration that causes 50% inhibition | (mg/L) |
| β | Biodegradation proportionality factor | (μ M/hr.K) |
| T | Absolute temperature | (K) |
| E_a | Activation energy | (kcal/mol) |
| R | Gas constant | (1.987×10^{-3} kcal/mol.K) |
| ΔS | Entropy change of enzyme deactivation | (kcal/mol.K) |
| ΔH | Enthalpy change of enzyme deactivation | (kcal/mol) |
| m/z | Mass-to-charge Ratio | |

1. INTRODUCTION

The rapid growth of the world's population and obligations to meet its requirement in recent decades have led to a significant increase in the consumption of pharmaceutically active compounds (PhACs) and their release into the environment (Khetan and Collins 2007). The research on the occurrence, fate and adverse effects of pharmaceuticals and their transformation products found in the environment has been trending up in recent years due to the implications of those compounds on human and environmental health. The major pathways of PhACs release into the environment are from drug manufacturing facilities, consumer use and inappropriate disposal of used and unused medicines, treatment of animals and hospital waste which eventually ended up in soil and aquatic environments. Additionally, PhACs are mainly excreted in urine or faeces, and then enter municipal wastewater treatment plants in which they may subject to biological, chemical and/or photochemical degradation. Depending on the environment they are present, different transformation processes can take place, some of which may produce even more persistent and toxic intermediates than parent compounds (Farre et al. 2008). As a consequence, these emerging micropollutants and their metabolites have been frequently detected in domestic and industrial wastewater, surface and groundwater, and soil throughout the world which threatens both human and environmental health (Heberer 2002, Stackelberg et al. 2004, Fent et al. 2006, Joss et al., 2006).

Effluents of the wastewater treatment plants (WWTPs) have been considered as a major source of these emerging contaminants since treatment plants are not designed to remove micropollutants (Petrovic et al. 2003, Stackelberg et al. 2004, Clara et al. 2005). Although the detected concentrations are typically at trace levels ranging from ng/L to µg/L, they still pose a potential threat to the aquatic ecosystems, animals and humans (Kolpin et al. 2002, Huber et al. 2005, Khetan and Collins 2007).

Advanced oxidation processes have been widely used for the removal of pharmaceuticals in wastewaters (Ternes et al. 2003, Khetan and Collins 2007). Yet, the efficiency of these treatment processes is often limited by the low concentration of the contaminants (Lu and Huang 2009). In addition, the requirement of high energy and

reagent input, and the generation of secondary pollutants make these methods undesirable (Li et al. 2007, Chen et al. 2010).

On the contrary, biodegradation is considered as an important environmental-friendly process for eliminating the majority of xenobiotics, including pharmaceuticals only if the toxicity of the compounds does not inhibit microbial activity (Barra Caracciolo et al. 2015). Some microorganisms are capable of utilizing pharmaceuticals as carbon and energy source via metabolic pathways, and converting them to easily metabolizable substrates (Wu et al. 2012). For example, members of the genus *Rhodococcus* and *Pseudomonas* are known for their ability to metabolize aromatic compounds of environmental concern (Zhang et al. 2013, Ivshina et al. 2006). Similarly, species of *Klebsiella pneumoniae* and *Bacillus subtilis* commonly exist in soils and have the ability to degrade phenolic compounds (Aravindhan 2014, Kadakol et al. 2010).

Moreover, enzymes have attracted attention as a way to deal with the PhACs removal since they are well-known biocatalysts (Touahar et al. 2014). Enzyme immobilization technique has provided catalytic transformation of many industrial toxic compounds, such as phenols (Liu et al. 2002) and anilines (Husain and Ulber 2011). Common immobilization methods are; adsorption or covalent binding onto a surface, encapsulation, entrapment into a polymer, and cross-linking (Bickerstaff 1997). An economical and simple method to immobilize enzymes is entrapment into calcium alginate (Ca-alginate) beads (Sakarya 2015). Even though enzymes may be efficient biocatalysts for the removal of PhACs, the low stability towards chemicals or thermal denaturation, short lifetime, high price, difficulty in recycling and time-consuming synthesis of enzymes can limit its applications in wastewater treatment (Touahar et al. 2014).

Acetaminophen (APAP), better known as paracetamol, is one of the most widely used antipyretic and analgesic drug all over the world. As a result, it has been identified as one of the most frequently detected anthropogenic compounds in aquatic environments generally within a concentration range from ng/L to µg/L (Khetan and Collins 2007, De Gusseme et al. 2011).

Microorganisms play a major role in aerobic APAP biodegradation in the environment (Wu et al. 2012). De Gusseme et al. (2011) isolated strains of *Delftia tsuruhatensis* and *Pseudomonas aeruginosa* that can degrade APAP in a membrane bioreactor doing nitrification. Zhang et al. (2013) investigated APAP biodegradation by pure cultures of three bacteria that belong to *Stenotrophomonas* and *Pseudomonas* genera as well as their consortium. That study showed that APAP biodegradation was faster by the consortium than individual microorganism. Hu et al. (2013) isolated a strain of *Pseudomonas aeruginosa* from a sequencing batch reactor treating APAP-contaminated wastewater. Liang et al. (2016) investigated APAP transformation in a soil/water system by isolating three bacteria from soil. They were assigned to the genus of *Bacillus* and *Klebsiella*.

Xu et al. (2015) investigated APAP biotransformation by using immobilized horseradish peroxidase (HRP) on poly(vinyl alcohol)/poly(acrylic acid)/SiO₂ (PVA/PAA/SiO₂) nanofibrous membranes (PPSiNFM-HRP). APAP removal efficiency of PPSiNFM-HRP was 83.5% with a rate of 0.023 min⁻¹. Touahar et al. (2014) studied biotransformation of a PhACs cocktail containing APAP by using both free enzymes and combined cross-linked enzyme aggregates (Combi-CLEAs) of oxidative enzymes, i.e. laccase (Lac) *Trametes versicolor*, versatile peroxidase (VP) from *Bjerkandera adusta* and glucose oxidase (GOD) from *Aspergillus niger*. APAP removal efficiency in a PhACs cocktail using free Lac, VP and GOD (alone or in combination) in the presence and absence of glucose (0.7 mM), peroxide (0.1 mM) and manganese sulfate (7 mM) for a contact time of 14 hours at room temperature and pH 5, was more than 95%. Also, Georgieva et al. (2010) obtained similar results for the removal of APAP by using an immobilized laccase of *Trametes versicolor*. Similarly, Ba et al. (2014) studied APAP removal from real wastewaters using combi-CLEAs of fungal laccase and mushroom tyrosinase. According to their results, APAP transformation extents were between 80 and 100%.

In the literature, limited number of species degrading APAP was presented and the effect of different environmental conditions on APAP biodegradation was briefly elucidated. Especially, bacteria playing a role on the fate of APAP in soil have not been studied in detail. The objective of this study is to isolate bacteria that can degrade APAP

in the soil, identify APAP biotransformation pathways, evaluate the environmental factors affecting the biotransformation of APAP in liquid cultures and develop an advanced treatment technology utilizing immobilized enzymes of a predominant bacterial species, which is capable of degrading APAP, entrapped into Ca-alginate beads in a batch reactor.

2. LITERATURE SURVEY

2.1. APAP in General

Acetaminophen (APAP), also known as paracetamol, with a IUPAC name of *N*-(4-hydroxyphenyl) ethanamide, which consists of three functional groups including hydroxyl group (OH), amide group (HN-CO-R) and aromatic group (benzene ring), is an active ingredient of antipyretic and analgesic drug, widely used for the treatment of headaches, fever and other minor pain worldwide. (Figure 2.1) As a result, it is frequently detected in wastewater and considered as an emerging micropollutant (Wu et al. 2012).

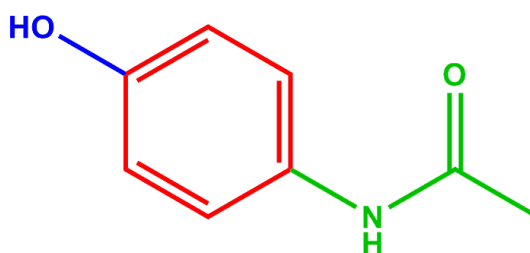


Figure 2.1. Molecular structure of Acetaminophen

Acetaminophen is available in a number of ways such as tablets, capsules, paediatric oral solutions, intramuscular and effervescent forms and can be bought in many different formulations as a mixture with other active ingredients such as codeine and caffeine.

Acetaminophen is an odorless, white crystalline compound, which is also very weak acid (pK_a of 9.38), exists as a neutral PhACs (Maeng et al. 2011) at neutral pH (NCBI Database, 2016) and has very low hydrophobicity ($\log K_{ow}$: 0.46) (NCBI Database, 2016). In water, its solubility is 14000 mg/L at 25 °C (NCBI Database, 2016).

APAP has ranked as one of the top three drugs prescribed in England, and has been one of the top 200 prescriptions in the US (De Gusseme et al. 2011). According to a recent report (Zion Research) which covers forecast and analysis for the acetaminophen market on a global and regional level and provides data of 2014 along with a forecast from 2015 to

2020, the annual global consumption of APAP is approximately 149,300 tons in 2014. The US accounts for about 40% of world demand.

Following oral administration, about 90% of APAP in the organism is metabolized primarily in the liver into glucuronide (about 52-57%) and sulphate (about 30-44%) conjugates. About 5-10% of the drug is oxidized to highly reactive cytotoxic metabolite *N*-acetyl-*p*-benzoquinone imine (NAPQI) via the hepatic cytochrome P-450 microsomal enzyme. NAPQI is detoxified by conjugation with glutathione and excreted in the urine as cysteine and mercapturic acid (Zhou et al. 2005, Mazaleuskaya et al. 2015). About 90-100% of an ingested dose is excreted in urine during about 24 hours. At therapeutic dosage, acetaminophen is excreted as glucuronide (45-55%), sulfate (20-30%), and cysteine (15-55%) conjugates. Approximately 3-5 % of acetaminophen is excreted unmetabolized by kidneys (Santos et al. 2013).

2.2. Occurrence of APAP in the Environment

Acetaminophen (APAP) has been identified as one of the most frequently detected anthropogenic emerging micropollutant in domestic and industrial wastewater, surface water and soil, as a result of its continuous release into the environment through effluents of drug manufacturing industries, consumer use and disposal, and hospital waste. APAP in the environment generally have a concentration ranging from ng/L to µg/L (Khetan and Collins 2007, De Gusseme et al. 2011).

Removal of APAP from WWTPs has been reported in some studies (Verlicchi et al. 2012). Removal efficiency varies from almost complete (>99%) to 86% in municipal and 80% in hospital WWTPs (Gomez et al. 2007, Radjenovic et al. 2009, Rosal et al. 2010, Boleda et al. 2011, Stackelberg et al. 2004, Ba et al. 2014, Kosma et al. 2014, Sui et al. 2015).

On the other hand, occurrence of APAP in both WWTPs effluents and surface waters was frequently reported. APAP has been detected at concentrations ranging from 59 to 220 ng/L in European WWTPs effluents (Pal et al. 2010). Gros et al. (2012) has found concentrations up to 338 ng/L in WWTPs effluent in Spain. In hospital effluents and

WWTPs influents, APAP concentrations can exceed 150 µg/L (Wu et al. 2012). APAP has been reported in 24% of surface waters in US with a median concentration of 110 ng/L and a maximum concentration of 10 µg/L (Kolpin et al. 2002). About 13% of surface and subsurface samples in US, APAP concentration varies in a range of 2.1-12.3 ng/L (Conley et al. 2008). Grujic et al. (2009) detected APAP within concentrations of 78-610 ng/L in 15% of surface or groundwater samples in Serbia. Similarly, APAP concentrations in surface waters was reported in Spain (12-30 ng/L) (Pedrouzo et al. 2007) up to 250 ng/L (Gros et al. 2006), in South Korea (4.1-73 ng/L) (Kim et al. 2007), in France up to 71 ng/L (Vulliet et al. 2011) and more than 65 µg/L in the Tyne River, UK (Kolpin et al. 2002, Roberts and Thomas 2006, Gros et al. 2006). In Europe, APAP concentrations ranging from 12 to 777 ng/L in freshwaters (rivers, canals) was reported by Pal et al. (2010). Moreover, Fram et al. (2011) reported APAP concentrations up to 1.89 µg/L in groundwater used for public drinking water supply in California. Similarly, Rabiet et al. (2006) detected 211 ng/L in a number of reservoirs used for drinking water supply. APAP has also been found in marine waters, with concentration levels up to 3 µg/L in the Aegean Sea and Dardanelles, as reported by Nödler et al. (2014).

APAP concentration varies between 37-294 mg/L in wastewater produced from a facility synthesizing APAP (Dalgic 2013).

Presence of APAP in water used as drinking water supplies is a concern when chlorination is used for disinfection since APAP reacts with chlorine to form several halogenated and oxidation products (Bedner and MacCrehan 2006, Glassmeyer and Shoemaker 2005), including the toxic compounds 1,4-benzoquinone and N-acetyl-p-benzoquinone imine (NAPQI) and two ring chlorination products, chloro-4-acetamidophenol and dichloro-4-acetamidophenol (Bedner and MacCrehan 2006).

APAP has been considered as a readily biodegradable compound with a reported half-life of 20 days (Bouissou-Schurtz et al. 2014). APAP can be removed from wastewater at high removal efficiency approximately over 99% (Santos et al. 2013, Chonova et al. 2016). Although APAP is relatively hydrophilic ($\log K_{ow} = 0.46$) which suggests that it is unlikely to adsorb to solid matrixes in biological treatment systems (Lin et al. 2010, Bouissou-Schurtz et al. 2014, Komesli et al. 2015), considerable amounts of APAP sorbs onto the

sludge in all WWTPs according to the study done by Komesli et al. (2015). Similarly, Albero et al. (2014) reported that some biosolids contained APAP at concentrations ranging between 24 to 290 $\mu\text{g}/\text{kg}$, as well.

APAP is not highly persistent in the environment (Santos et al. 2013). Once entered in the environment, it is mainly degraded by microorganisms, which are capable of using APAP as carbon and energy source for their metabolic activities (Wu et al. 2012). However, continuous release of APAP and its transformation products to water bodies, where they interact with aquatic organisms, confront us with their fate and potential threat to the environment. Undoubtedly, they can adversely affect the balance of aquatic ecosystems and all organisms having an interaction with those ecosystems, even at low concentrations (Huber et al. 2005).

2.3. Ecotoxicity of APAP

APAP has an estimated $\log K_{ow}$ of 0.46 and a bioconcentration factor (BCF) of 3, which suggest that potential for bioconcentration in aquatic organisms is low (Bouissou-Schurtz et al. 2014).

APAP affects reproduction in daphnia or fish embryonic development at environmentally relevant concentrations (Bouissou-Schurtz et al. 2014). Galus et al. (2013a, b) reported increased mortality and developmental abnormalities, such as spinal malformations or pericardial oedema, in zebrafish after embryonic exposure to APAP at a level of 0.5 $\mu\text{g}/\text{L}$, which is close to the environmental concentrations found in the French national water survey (0.443 $\mu\text{g}/\text{L}$) (ANSES, 2011). According to a study done by Kim et al. (2012), APAP could alter sex hormone balance, leading to increased vitellogenesis in male fish. Indeed, APAP exposure between 0.095 $\mu\text{g}/\text{L}$ to 95 $\mu\text{g}/\text{L}$ resulted in concentration-dependent increases of hepatic vitellogenin protein, confirming endocrine disruption (Kim et al., 2012).

According to Parolini et al. (2010), APAP at environmentally relevant concentrations (0.75-1.51 $\mu\text{g}/\text{L}$) induced moderate cyto-genotoxicity in freshwater bivalve zebra mussel (*Dreissena polymorpha*). These authors explained this genetic damage as the increase in

oxidative stress and/or a direct interaction between its highly reactive metabolite NAPQI with proteins and nucleic acids. In addition, this electrophilic intermediate can increase the formation of Reactive Oxygen Species (ROS) and Reactive Nitrogen Species (RNS), such as superoxide anion, hydroxyl radical, hydrogen peroxide, nitro oxide and peroxyxynitrite, then which can react and create broad injuries to DNA.

The study done by Nunes et al. (2014a) demonstrated that APAP is toxic to *Vibrio fischeri*, *Pseudokirchneriella subcapitata*, *Cylindrospermopsis raciborskii*, *Daphnia longispina*, *Daphnia magna*, *Lemna minor* at concentrations ranging between 1.7 mg/L to 1000 mg/L, except for *Lemna gibba*, which exhibited no effects at concentrations up to 1000 mg/L. Moreover, APAP was more toxic to the two crustacean species (*D. magna* and *D. longispina*), than primary producers (the algal species and the two selected macrophytes). APAP at concentrations above 1.7mg/L caused significant impairments of offspring production and population growth potential in daphnids, which means APAP causes oxidative stress which facilitates endocrine disruption as mentioned by Kim et al. (2012). Although APAP shares structural similarities with a well-known family of endocrine disruptors in crustaceans (Rodriguez et al. 2007), further research is needed to clarify whether APAP elicit endocrine disruption in crustaceans. Nunes et al. (2014a) also explained the differences in acute toxicity values of APAP among organisms, even they share some phylogenetic similarity in terms of differences in the nutritional status of test organisms. Similarly, increased toxic effects of APAP for humans can be related to nutrient deficits (Berling et al. 2011), since nutrients can affect glutathione metabolism which is the main APAP biotransformation pathway in mammalian species. Generally, low levels of APAP do not result in any cellular damage, since it is conjugated with glucuronide and sulphate in mammalian species (Xu et al. 2008). The excretion of NAPQI prevents the occurrence of oxidative stress and cellular damage. However, high doses of APAP can cause an increase in the formation of NAPQI and its consequent toxic effects, which include covalent modifications of thiol groups of cellular proteins (Xu et al. 2008), DNA and RNA damage, and oxidation of membrane lipids, resulting in necrosis and cellular death (Hinson et al. 2004). The metabolism of APAP is also responsible for the formation and release of reactive oxygen species, in other organisms, such as fish (Ramos et al. 2014), mollusks and crustaceans (Antunes et al. 2013, Brandão et al. 2014, Parolini et al. 2009). As Sarma et al. (2014) indicated, the overproduction of reactive oxygen species

by APAP metabolism was connected to the oxidative stress response in organisms, thus capable of altering population traits in crustacean species.

Gómez-Oliván et al. (2012) reported that APAP induced oxidative stress in the amphipod species *Hyaella azteca*. Correia et al. (2016) described the deleterious effects of APAP on the clam species *Ruditapes philippinarum*, regarding oxidative stress defense/metabolism, under varied conditions of salinity.

Kummerova et al. (2016) described the effects of APAP at environmentally relevant concentrations in freshwater aquatic plant, *Lemna Minor*. According to this research, APAP caused an increase in ROS and RNS in roots which resulted in a decrease in metabolic activity of the cells and a decrease in photosynthetic pigments chlorophyll(a), chlorophyll(b), and carotenoids content at concentrations between 10 and 100 µg/L. APAP exhibited acute toxicity in *Eisenia fetida*, an earthworm, at concentrations above LC₅₀ of 693.50 mg/kg (Pino et al. 2015).

Bartha et al. (2010) investigated APAP in terms of fate, detoxification and effect on defense mechanisms in one of the hydroponically grown phytoremediation plant species, Indian mustard (*Brassica juncea*). APAP detoxification in plant tissues, in which APAP conjugates with glutathione and glucose, exhibited strong similarities to the mammalian metabolism. These authors also indicated that APAP at high concentrations over 1 mM caused strong damages in the root, along with oxidative stress and irreversible damages in the plants. Yet, visual symptoms and morphological changes like brownish discoloration and inhibited root growth were also observed.

Proia et al. (2013) investigated the effects of APAP on the structure and function of biofilms in Llobregat River in Barcelona, Spain. APAP was shown to favor growth in cyanobacteria while having a negative effect on growth in green algae.

Study done by Johnston et al. (2002) shows that APAP-mouse baits are readily consumed by and acutely toxic to the invasive brown tree snakes (*Boiga irregularis*) in Guam. However, non-target wildlife species including include feral dogs and cats, wild pigs (*Sus scrofa*), small rodents, monitor lizards (*Varanus indicus*), crabs, and the

endangered Mariana crow and Guam rail (*Gallirallus owstoni*) could also be exposed to APAP by direct consumption of the treated mouse baits and/or by the consumption of dead or dying snakes poisoned by APAP. For all species, hazard quotients (HQ) greater than 0.5 suggest that there may be significant risk to non-target species associated with the proposed use of a chemical. For endangered species, HQ greater than 0.1 suggests that the non-target risks associated with the use of the chemical may be unacceptable to regulatory agencies such as the US EPA.

2.4. Biodegradation of APAP

Biodegradation is the primary natural mechanism responsible for APAP removal in the environment (Yamamoto et al. 2009, Lin et al. 2010, Verlicchi et al. 2012, Santos et al. 2013, Bouissou-Schurtz et al. 2014, Barra Caracciolo et al. 2015).

Yu et al. (2011) investigated the biodegradability and biosorption of APAP on immobilized cells. According to their findings, 99% of APAP was adsorbed on the biomass-carrier complex whereas about 25% sorbed APAP was degraded within 2 days.

Lam et al. (2004) investigated biodegradation of eight pharmaceuticals in a microcosm study and reported a half-life ($t_{1/2}$) of 0.9 ± 0.2 days for APAP. Yamamoto et al. (2009) reported that 96% of APAP was degraded in activated sludge with a half-life of 50 hours. Similarly, Lin et al. (2010) reported a half-life ($t_{1/2}$) of 2.1 days for APAP biodegradation in lab-scale aqueous environment. Additionally, earlier studies which investigated the sorption of APAP by aquifer sand, silica, and alumina (Lorphensri et al. 2006), indicated that sorption to those media is negligible, therefore biodegradation is the major mechanism for APAP removal in the environment. Ranieri et al. (2011) carried out APAP removal in subsurface flow constructed wetlands, planted with two different macrophytes (*Phragmites australis* and *Typha latifolia*) and found out APAP removal was caused by biodegradation than the sorption which might be related to the biofilm development in the roots. A study done by Escapa et al. (2015) was carried out to assess the bioremediation potential of the microalgae *Chlorella sorokiniana* to remove APAP from water. Efficiencies of APAP removal at the end of the batch culture were found more than 67%. de Wilt et al. (2016) also investigated the removal of APAP in batch

experiments with the microalgae *Chlorella sorokiniana* grown in urine, anaerobically treated black water and synthetic urine. Their algal treatment system achieved 99% of APAP removal in all batch reactors.

Anaerobic biodegradation of APAP by methanogenic bacteria has been studied by Musson et al. (2010). According to their results, APAP concentrations in biologically active samples showed a decrease up to 11%, suggesting that anaerobic degradation of APAP was not significant.

Aerobic bacteria play a major role in APAP biodegradation in the environment (Wu et al. 2012). A *Penicillium species* were isolated by Hart and Orr (1975), from an acidic APAP solution and identified as the first-APAP degrader in the literature. Bacterial species that can degrade APAP are predominantly assigned to the genera of *Pseudomonas*, *Rhodococcus* and *Bacillus*. APAP biodegradation by pure cultures of *Rhodococcus* species, which is gram-positive Actinobacteria was investigated by Ivshina et al. (2006). Sixty-four strains tested belonged to six species of *Rhodococcus erythropolis*, *Rhodococcus fascians*, *Rhodococcus "longus"*, *Rhodococcus opacus*, *Rhodococcus rhodochrous* and *Rhodococcus ruber*, all of which were resistant to APAP. *Rhodococcus erythropolis* and *Rhodococcus ruber* were more resistant to APAP than the rest of the species tested. Among them, *Rhodococcus ruber* strain IEGM 77 was able to convert APAP to *p*-aminophenol, pyrocatechol, and hydroquinone.

De Gusseme et al. (2011) isolated strains of *Delftia tsuruhatensis* and *Pseudomonas aeruginosa* that can utilize APAP completely in a membrane bioreactor (MBR) inoculated with an enriched nitrifying culture. During APAP degradation by the two isolates a brown coloration was observed, which might be related to the accumulation of certain transformation products, such as catechol. In addition, hydroquinone, which is in equilibrium with 1,4-benzoquinone, identified as the main biotransformation product. As indicated by (Bedner and MacCrehan 2006) 1,4-benzoquinone is a benzene metabolite exerting genotoxic and mutagenic effects and might impose an environmental concern. However, biotransformation products were further degraded.

Zhang et al. (2013) investigated the APAP biodegradation by pure cultures of three bacteria that belong to *Stenotrophomonas* and *Pseudomonas* genera as well as their co-culture. *Stenotrophomonas* sp. f1, *Pseudomonas* sp. f2, and *Pseudomonas* sp. fg-2 demonstrated complete APAP degradation at concentrations up to 400, 2500 and 2000 mg/L, respectively. Nevertheless, degradation and mineralization of APAP was faster by the consortium than individual microorganism. In addition, *p*-aminophenol and hydroquinone were identified as two key metabolites, along with other intermediates five carboxylic acids (2-hexenoic acid, succinic acid, malonic acid, formic acid and oxalic acid) and two inorganic ions (nitrate and nitrite) for isolated strains in their study. Biotransformation mainly proceeded via *p*-aminophenol to hydroquinone.

Hu et al. (2013) isolated a strain of *Pseudomonas aeruginosa* HJ1012 from a microbial aggregate in a sequencing batch reactor (SBR) treating APAP-contaminated wastewater. This strain was shown to degrade APAP up to 2200 mg/L with a high mineralization potential about 71.4%. Hydroquinone and *p*-aminophenol have been detected as the main intermediates, along with four saturated carboxylic acids (formic acid, oxalic acid, lactic acid and succinic acid) and two inorganic ions (nitrate and nitrite).

Liang et al. (2016) carried out APAP transformation in a soil/water system by isolating three bacteria, which were assigned to the genus of *Bacillus* and *Klebsiella*, from soil. The main transformation product was identified as *p*-aminophenol, followed by the formation of hydroquinone and 1,4-benzoquinone. Li et al. (2014) elucidated APAP degradation pathways in soil, with an emphasis on the identification of degradation intermediates including 3-hydroxyacetaminophen, hydroquinone, 1,4-benzoquinone, *N*-acetyl-*p*-benzoquinone imine, *p*-acetanisidide, 4-methoxyphenol, 2-hexenoic acid, and 1,4-dimethoxybenzene.

The main objective of this research is to identify active APAP degraders in soil and evaluate mechanism of APAP biodegradation. In the course of this research, novel APAP degraders were isolated from an enrichment microbial community developed from a soil sample, environmental factors affecting APAP biodegradation were evaluated and biodegradation of APAP with immobilized cells of an APAP-degrader was assessed.

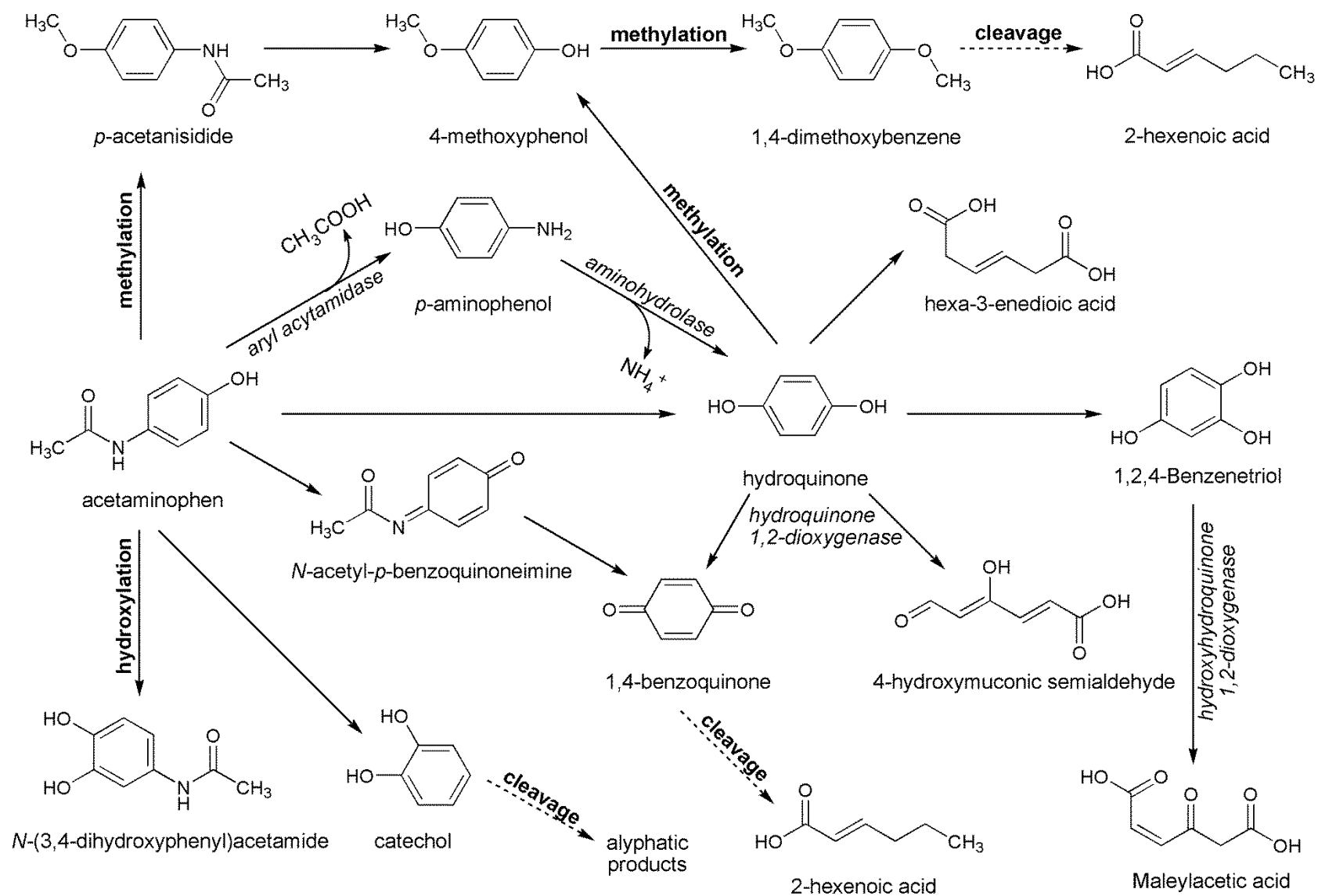


Figure 2.2. Proposed pathway of APAP biotransformation from the previous studies

3. MATERIALS AND METHODS

3.1. Chemicals

Acetaminophen (APAP, $C_8H_9NO_2$, 151.165 g/mole) was obtained in high purity from Sigma-Aldrich (St. Louis, MO, USA) and all other chemicals used in mineral salt medium preparations, SDS-PAGE experiment and organic solvents used in experiment and instrumental analysis were obtained from Merck, Sigma-Aldrich, Bio Basic Inc. or Bio-Rad Laboratories Chemicals Company.

3.2. Development of APAP Degrading Soil Microbial Community

A soil sample was taken close to the rizosphere of a tree located in Bogazici University Hisar Campus garden, Istanbul. Two grams of sample was aseptically transferred into 198 mL of salt medium composed of 740 mg/L K_2HPO_4 , 300 mg/L KH_2PO_4 , 50 mg/L NaCl, 100 mg/L NH_4Cl , 25 mg/L $MgSO_4 \cdot 7H_2O$, 1.5 mg/L $CaCl_2 \cdot 2H_2O$, 0.2 mg/L $FeCl_3 \cdot 6H_2O$, 0.05 mg/L $ZnCl_2$, 0.03 mg/L $MnCl_2 \cdot 4H_2O$, 0.3 mg/L H_3BO_3 , 0.2 mg/L $CoCl_2 \cdot 6H_2O$, 0.01 mg/L $CuCl_2 \cdot 2H_2O$, 0.02 mg/L $NiSO_4 \cdot 6H_2O$, 0.03 mg/L $Na_2MoO_4 \cdot 2H_2O$ and amended with 50 mg/L APAP as the only carbon and energy source in a 500-mL glass bottle with a screw-cap. The reactor was incubated at 22°C room temperature on a rotary shaker at 130 rpm. APAP concentration in the bottle monitored at appropriate time intervals using HPLC method described below. As soon as all APAP was utilized, 20 mL sample taken from the bottle was transferred aseptically into a new bottle containing 180 mL fresh medium and 50 mg/L APAP. This enrichment step was repeated for 2 more times after APAP was utilized in each time.

3.3. Isolation of APAP Degraders in the Enrichment Community

After a specialized APAP degrading community was established, 100 μ L of appropriately diluted sample taken from the bottle was spread on CHROMagarTM Orientation plate which was prepared by adding of 8.25 g of OR agar into 250 mL DI water followed by stirring and boiling the mixture on a hot plate.

After one day incubation at 30°C, 37 colonies were picked up and purified by streaking on Luria-Bertani (LB) agar containing 10 g tryptone, 5 g yeast extract, 5 g NaCl and 15 g agar in 1 L water. Colonies obtained after purification were inoculated into 10-mL culture tubes containing 2 mL salt medium with 50 mg/L APAP and incubated at 22°C room temperature. APAP concentration in the tubes was monitored using an HPLC method described below. The isolates having the ability to consume APAP in the tubes were assigned as APAP degraders.

3.4. Identification of APAP Degraders Based on 16S rRNA Gene

Genomic DNA of those 28 APAP-degrading isolates was extracted. Extracted genomic DNA of each isolate was confirmed on 0.7% agarose gel and quantified using Implen® P360 NanoPhotometer (Implen GmbH, Munchen, Germany). 16S rRNA gene of each isolate DNA was amplified by PCR using TaKaRa Premix TaqTM Kit (TaKaRa Bio, Shiga, Japan) with 27F (5'-AGAGTTTGATCMTGGCTCAG-3') (0.4 µM), and 1492R (5'-TACGGYTACCTTGTTACGACTT-3') (0.4 µM) primers. PCR conditions included 35 cycles at 94 °C (30 sec), 55 °C (30 sec) and 72 °C (1min), with a final extension at 72 °C for 7 min. Amplified 16S rRNA was electroporated on 1% Agarose gel (SeaKem LE Agarose, Lonza Inc., Basel, Switzerland), stained with PronaSafe, UV-illuminated (GelDOC EZ, BioRad, CA) and purified using EZ-10 PCR Purification Kit (Bio Basic Inc., Ontario, Canada). Purified 16S rRNA sample of the isolate was sequenced by MacroGen Inc. Europe (Amsterdam, Netherlands). Forward and reverse sequences were trimmed and assembled using Geneious Software (Biomatters Ltd., Auckland, New Zealand) to yield about 1250 bp length and above 95% quality 16S rRNA sequence. The sequence was then queried against the NCBI database using MEGABLAST algorithm and closest neighbor sequence to queried sequence was determined. Phylogenetic relationship between our isolates, 3 closest bacteria to our isolates and other APAP-degrading species in the literature was performed using Geneious Software (Biomatters Ltd., Auckland, New Zealand) following appropriate alignment and tree building algorithms.

3.5. LB Growth Assay

Specific growth rate and optimum growth temperature for the most abundant APAP degrader isolated from the community were determined as follows: 1.5 mL overnight grown culture sample was well agitated and transferred into 98.5 mL sterile LB broth in Erlenmeyer flasks. The flasks were incubated at 5, 10, 15, 22, 30, 35, 40 and 45°C. At appropriate time intervals, 1 mL of sample was taken and optical density (OD) was measured with Implen® P360 NanoPhotometer (Implen GmbH, Munchen, Germany) at 600 nm wavelength. 98.5 mL sterile LB broth without culture was used as control. Specific growth rate (μ) and doubling time (t_d) at each temperature was calculated using the following equations (Eq. 3.1 and 3.2);

$$\frac{dOD}{dt} = \mu OD \quad (3.1)$$

$$\mu = \frac{0.693}{t_d} \quad (3.2)$$

3.6. Kinetic Assays

A set of biotransformation assays were performed at different biophysicochemical conditions to determine optimum conditions for APAP biotransformation by the *Rhodococcus erythropolis* BIOMIG-P19 isolate. All assays were performed using the following procedure: Kinetic experiments were performed in 100-mL Erlenmeyer flasks. 1.5 mL of overnight grown culture of selected isolate was transferred into 20 mL salt medium containing 10 mg/L initial APAP concentration to maintain c.a. 1×10^{11} CFU/L initial cell density in the flasks. Each flask was agitated on an orbital shaker at 130 rpm at 22°C room temperature. As soon as APAP was consumed, the flasks were re-spiked with a desired APAP concentration. Samples were taken from each flask and APAP concentration was measured with HPLC at certain time intervals during the course of incubation. Flasks prepared exactly the same way described above but containing no microorganisms were used as controls and monitored in the course of incubation. All flasks were prepared in triplicate. A control flask was prepared exactly the same way but without microorganisms to examine the abiotic substrate loss. All the experiments were performed in triplicate.

APAP biotransformation was simulated using Michaelis-Menten growth model (Equation 3.3) (Rittmann and McCarty 2001):

$$\frac{d[APAP]}{dt} = \frac{k [APAP] X}{K_{APAP} [APAP]} \quad (3.3)$$

where; $[APAP]$ is APAP concentration (mg/L); k is cell specific rate of APAP utilization (mg/cell.h); K_{APAP} is half-saturation constant (mg/L); X is cell density (cells/L).

Eqn-3 was fitted to experimental data to estimate k and K_{APAP} values of APAP biotransformation by selected isolate using Berkeley-Madonna software following error minimization employing Runge-Kutta 4 integration method. All the k (mg/cell.h) values reported in this thesis can be converted to observed rate constant (k' , mg/L.hr) by multiplying k with 10^{11} CFU/L.

3.7. Oxygen Threshold Concentration for APAP Biotransformation

The O₂ threshold concentration for APAP biotransformation by the selected isolate was performed in a closed 120-mL serum bottle. The bottle was sterilized and filled with 100 mL salt medium containing the isolate at 1×10^{11} CFU/L. The bottle was closed with a rubber stopper and sealed with an aluminum cap. Bottle was incubated for 3 days at room temperature in order to confirm that all residual organics in the media had been depleted. At the third day, the bottle was spiked with 100 mg/L APAP concentration. APAP was monitored with HPLC and headspace oxygen and carbon dioxide were monitored with a GC unit (Figure 3.1).

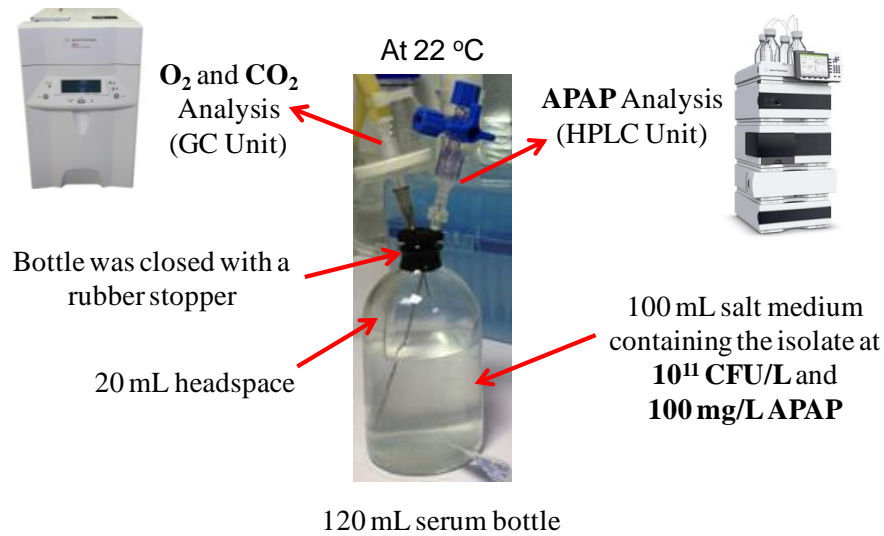


Figure 3.1. Closed bottle set-up used for determining APAP biotransformation under limiting O₂ concentration

3.8. APAP Biotransformation Kinetics using Crude Enzymes of BIOMIG-P Cells

Enzyme kinetic experiments were performed in 1.5 mL HPLC vials containing ≈ 0.5 mg protein and 10 mg/L APAP concentration in each vial. Ten mL of overnight grown culture of BIOMIG-P cells were transferred into 10 mL salt medium containing 100 mg/L initial APAP concentration. Each flask was agitated on an orbital shaker at 130 rpm at 22°C room temperature. As soon as APAP was consumed, content in each flask was centrifuged and resuspended in 1 mL salt medium. 1 mL of cell suspensions were centrifuged again and tubes containing pellets were grinded in 10 second pulses for 1 min using grinder on an ice block and resuspended in 750 μ L salt medium. After centrifugation of each tube, supernatants containing proteins were transferred into clean tubes and protein concentrations of each tube were measured with Implen® P360 NanoPhotometer (Implen GmbH, Munchen, Germany). Certain amount of crude protein extracts of each BIOMIG-P cells were transferred into an HPLC vial to yield around ≈ 0.5 mg protein. Each vial was spiked with 10 mg/L APAP and the concentration of APAP was measured with HPLC at certain time intervals during the course of experiment.

3.9. Protein Extraction and SDS-PAGE

Two hundred mL of overnight grown culture of BIOMIG-P cells were transferred into 100 mL salt medium containing 100 mg/L initial APAP concentration. Each flask was agitated on an orbital shaker at 130 rpm at 22°C room temperature. As soon as APAP was consumed (\approx 7 hours), each cell was centrifuged and resuspended in 20 mL 10 mM MOPS (3-n-morpholinopropanesulfonic acid) medium. 10 mM MOPS was prepared by adding 2.1 g MOPS into 1 L DI water. The pH was then adjusted to 7.2 with 1 M NaOH (4 g NaOH in 100 mL DI water) and solution was autoclaved at 121°C for 15 min. Similarly, 200 mL of overnight grown culture of BIOMIG-P cells were centrifuged and resuspended in 20 mL salt medium but without containing APAP. 20 ml of cell suspensions were transferred into beakers, which were placed in an ice bath. Each cell suspension was sonicated by ultrasound with 10 min short burst of 10 seconds followed by 30 sec intervals for cooling in total of 4 minutes. Cell debris of each suspension was removed by ultracentrifugation at 4°C for 30 minutes at 12000 rpm using Beckman Coulter Allegra™ 64R Centrifuge. Protein concentration of each supernatant was estimated using nanodrop application of Implen® P360 NanoPhotometer. Protein suspensions were stored in -20°C until later analysis.

10% Separating gel mix was prepared by adding of 4.1 mL DI water, 3.3 mL 30% (w/v) Acrylamide/Bis, 2.5 mL 1.5 M Tris-HCl (pH 8.8) and 0.1 mL 10% SDS. After 15 min degassing of separating gel mixture via sonification, 50 μ L 10% (w/v) APS and 5 μ L TEMED were added to the solution and immediately poured between the plates leaving 1.0 cm for the stacking gel and comb. 5% stacking gel mix was prepared by adding of 5.7 mL DI water, 1.7 mL 30% (w/v) Acrylamide/Bis, 2.5 mL 0.5 M Tris-HCl (pH 6.8) and 0.1 mL 10% SDS. After 15 min degassing of separating gel mixture via sonification, 50 μ L 10% (w/v) APS and 10 μ L TEMED were added to the stacking gel mixture and immediately poured on top of separating gel. Comb was inserted between the glass plates and left for polymerization for 2 hours at 22°C room temperature. 10X electrophoresis (running) buffer, containing 25 mM Tris, 192 mM glycine, 0.1% SDS (pH 8.3), was diluted to 1X with deionized water. 2X Loading (Sample) Buffer containing 3.55 mL DI water, 1.25 mL 0.5 M Tris-HCl (pH: 6.8), 2.5 mL glycerol, 2 mL 10% SDS, 0.2 mL 0.5% (w/v)

Bromophenol Blue was prepared, and then 50 μL β -mercaptoethanol was added to the buffer prior to mixing with the samples.

SDS-PAGE Electrophoresis was carried out in 10% separating gel and a 5% stacking gel, with 1X running buffer. When polymerization of 10% separating gel was complete, 5% stacking gel was poured on top of separating gel. Combs were inserted between the glass plates and left for polymerization for 2 hours at room temperature. After polymerization of stacking gel, combs were removed and wells were filled with 1X running buffer. 15 μL Protein samples were mixed with 10 μL 2X loading buffer and heated at 95°C for 5 minutes using Agilent SureCycler 8800 Thermal Cycler. 25 μL of samples were cooled down on ice for 10 minutes and loaded onto the polyacrylamide gels along with 10 μL of protein ladder standard Precision Plus Protein™ Dual Xtra (Bio-Rad) which including 9 blue-stained bands, and 3 pink reference bands (2, 25, 75 kD). Electrophoresis was performed at room temperature in a vertical tank apparatus (Mini-PROTEAN® Tetra Vertical Electrophoresis Cell) maintained at 120V using a constant-voltage power supply (Bio-Rad PowerPac™ Universal Power Supply) for 1.45 hours, in which 25 kD reference band reached the bottom of the gel (Figure 3.2). At the end of electrophoresis, polyacrylamide gels were stained using Bio-Rad Coomassie Brilliant Blue R-250 Staining Solution and then destained by agitation in deionized water/methanol/acetic acid mixture (83:10:1 v/v) for 12 hours at room temperature. Protein band patterns were imaged on Bio-Rad Gel Doc™ EZ Imaging System using White Tray. Molecular weight analyses of proteins were evaluated with Image Lab™ Software 5.1.

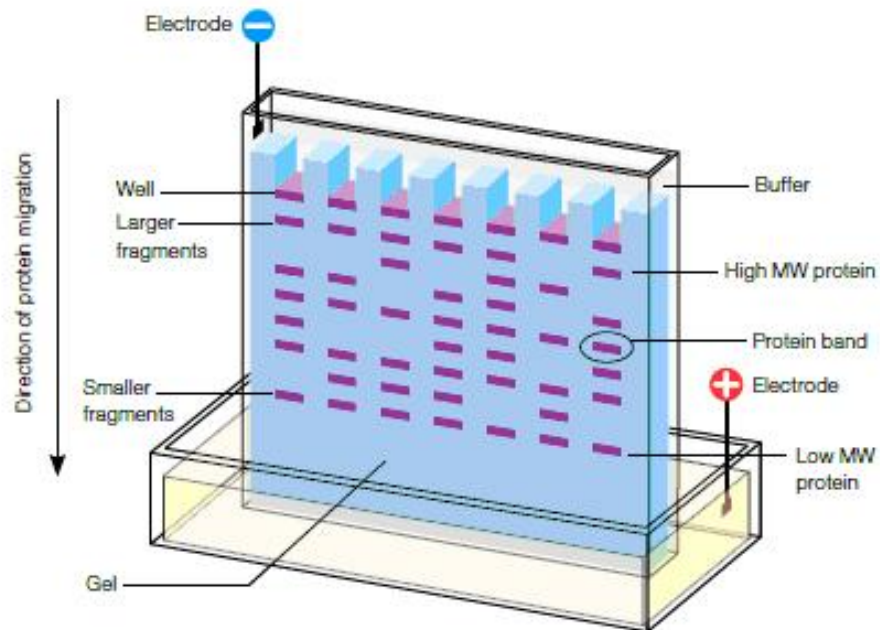


Figure 3.2. Schematic representation of SDS-PAGE setup (Bio-Rad Bulletin 6040 Rev B)

3.10. Ca-Alginate Bead Preparation

Beads with 3 mm diameter were synthesized via dripping 3% Na-alginate solution into 0.15 M CaCl_2 solution through a Pasteur pipette from a 20 cm height via peristaltic pump operated at 2.5 mL/min flowrate (Figure 3.3). After 40 minutes, the pump was stopped and the beads were separated from CaCl_2 solution via a Buchner funnel. For 3% (w/v) sterile Na-alginate preparation, 3 g Na-alginate was poured slowly into a bottle containing 100 mL DI water on a stirrer. After about 45 minutes the solution was taken into autoclave at 121°C for 15 min. 0.15 M CaCl_2 was prepared by addition of 22.1 g CaCl_2 into DI water. Sterilization of CaCl_2 solution was done by autoclaving at 121°C for 15 min. Beads on the funnel were washed with sterile 10 mM MOPS buffer, and added into 10 mM MOPS buffer with a sterile spoon. The beads in the solution were kept at +4°C. For the preparation of beads that contain BIOMIG-P19 enzymes, 20 mL enzyme solution was added into 80 mL Na-alginate solution under aseptic conditions. All the procedure was done under a laminar flow hood.



Figure 3.3. Ca-alginate bead preparation setup

3.11. Kinetic Experiments with Enzyme Beads

The protein concentration in the enzyme-entrapped beads was around 0.002 mg protein/bead. The APAP biotransformation kinetics of beads was investigated in two parallels and a control in 250-mL Erlenmeyer flasks using 3-mm beads synthesized in 0.15 M CaCl_2 . About 750 ± 20 (≈ 30 mL beads) 3-mm beads were transferred into Erlenmeyer flasks containing 70 mL 10 mM MOPS buffer and 10 mg/L initial APAP concentration. Flask containing beads but without enzymes were prepared as a negative control. Each flask was agitated on an orbital shaker at 30 rpm. Samples taken at appropriate intervals were measured using the HPLC method described below.

3.12. Analytical Methods

Acetaminophen was measured analyzed using Agilent Technologies 1260 Series High Performance Liquid Chromatography unit (HPLC) equipped with a Waters Nova-Pak C8 60Å column (4 μm , 3.9 mm x 150 mm). A 30:70 (v/v) mixture of methanol and deionized water was used as the mobile phase at a flow rate of 1.0 mL/min and the column is maintained at 35°C. Detection was obtained with a diode array detector at a wavelength range of 210-600 nm. The retention time of APAP which was quantified at a 243 nm under

these conditions was 1.63 min. An example of HPLC chromatogram of APAP in mobile phase was given in Figure 3.4.

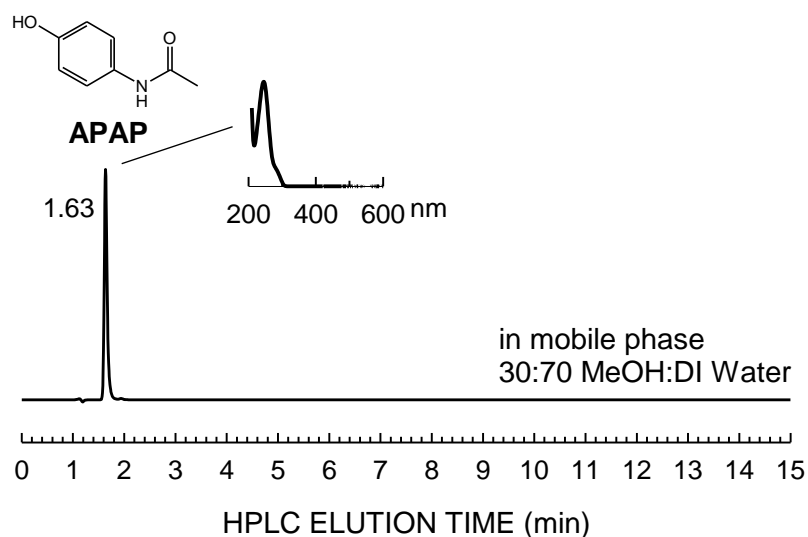


Figure 3.4. Sample HPLC chromatogram of APAP in mobile phase

The calibration curves of APAP were linear ($r^2 > 0.99$) within 1 mg/L and 100 mg/L (~6.62 μ M-661.54 μ M) (Figure 3.5).

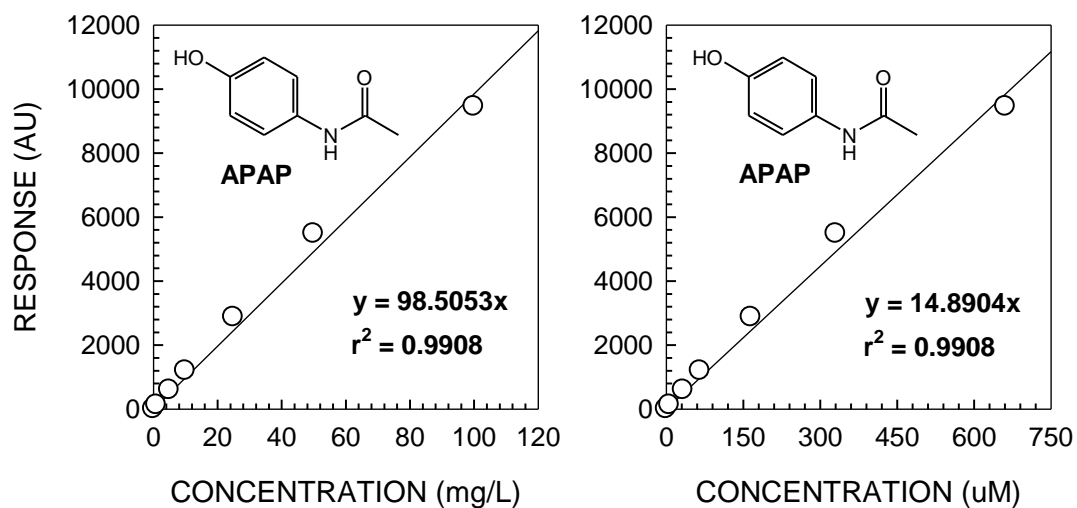


Figure 3.5. Mass and molar calibration curves of APAP

The head space O_2 and CO_2 in the bottles were determined by an Agilent 6850 Series GC unit (Agilent Technologies Inc., Palo Alto, CA) equipped with a 30 m Carboxen 1010 Plot fused silica, 0.53 mm i.d. column (Supelco Inc.) and a thermal conductivity detector.

Helium was used as the carrier gas at a constant flow rate of 6 mL/min. The 10:1 split injector was maintained at 150 °C, the oven was set at 40 °C and the detector temperature was set at 150 °C. All gas analyses were performed by injecting a 200 µL gas sample.

APAP biotransformation by-products were identified using an AB SCIEX QTRAP® 4500 LC-MS/MS system with Turbo V™ ion source and Electron Spray Ionization (ESI) probe in both positive and negative polarity. Nitrogen was used as the collision gas. The 100-fold diluted samples were analyzed by direct infusion into the ESI source via a syringe pump at a flow rate of 10 µL/min. Enhanced Mass Scanning (EMS) and Enhanced Product Ion (EPI) scan modes were used to acquire information on parent compounds and their fragmentation patterns, respectively. The mass spectrometer was operated in the following parameters, which were kept constant during the whole acquisition: Ion source Temperature: 500°C; Curtain Gas: 20 psi; Nebulizer Gas: 40 psi; Heater gas: 60 psi; CAD Gas: Low; IS pos: +5500 V. The EMS spectra of the samples were obtained by scanning over the m/z range from 55 to 155 at a scan rate of 10000 Da/s using collision energy (CE) at 10 V, declustering potential (DP) at 70 V and entrance potential (EP) at 10 V. EPI spectra were acquired at a scan rate of 10000 Da/s using dynamic fill at a Collision Energy (CE) of 35 V with a collision energy span (CES) of 15. All data were acquired and processed using the Analyst 1.6.2. Software. The characteristic MS/MS spectra patterns were searched against Human Metabolome Database (HMDB) Library and literature to confirm the fragmentation patterns. Daughter ions of the metabolites were interpreted. An example of EMS spectrum of APAP was given in Figure 3.6.

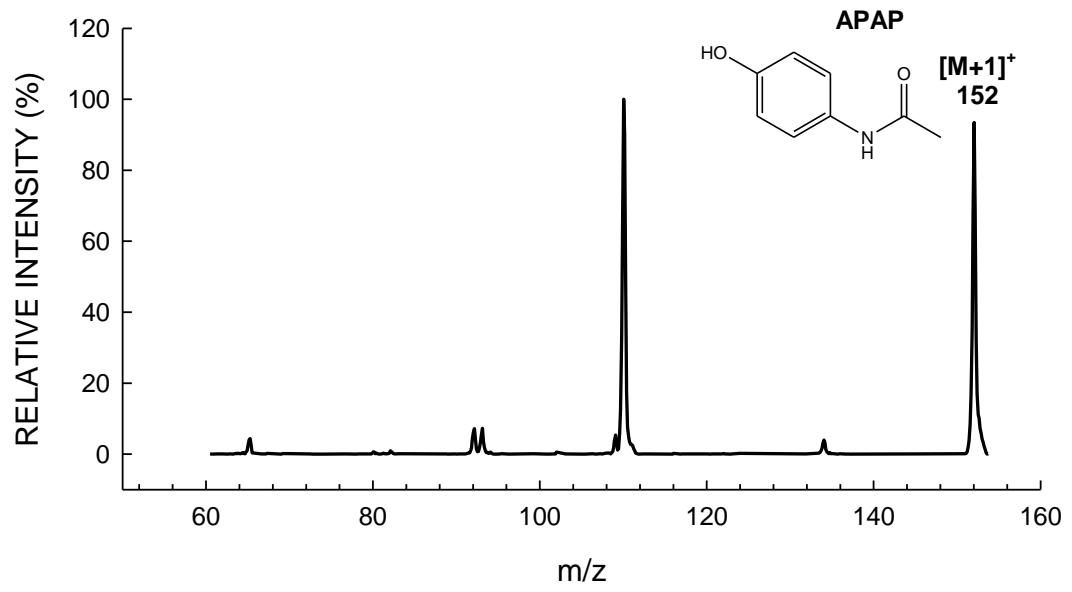


Figure 3.6. EMS spectra of APAP using DP at 56 V, EP at 10 V and CE at 23 V

4. RESULTS AND DISCUSSION

4.1. Activity of APAP Degrading Community

Acetaminophen was consumed at each enrichment round during culture development process through 25 days (Figure 4.1). APAP concentration did not change in the control bottle which was prepared without a soil inoculum. Therefore, the disappearance of APAP in the microbial community bottle during the course of experiment was attributed to biodegradation.

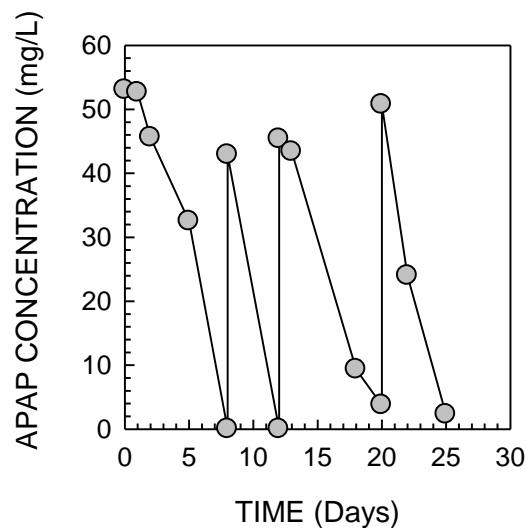


Figure 4.1. APAP degrading microbial community development

After a specialized APAP degrading community was established, chromogenic agar (CHROMagarTM OR) was used for determination of the biodiversity in the microbial community. According to this method, colonies of specific microorganisms can be distinguished by their color. However, in this study, all colonies were grown in beige color on CHROMagarTM OR. Same natural color produced for each colony on chromogenic agar can be explained by not belonging to the certain group of microorganisms previously described.

isolates determined by maximum likelihood followed by UPGMA tree building method and Jukes-Cantor genetic distance model, relative to other bacterial strains (● Acetaminophen degraders isolated in previous studies and ● this study)

Four out of 28 APAP-degrading colonies were identified as *Pseudomonas nitroreducens* BIOMIG-P2. 16S rRNA sequence of this strain was 100% similar to *Pseudomonas* sp. AC in the NCBI database (Figure 4.2). BIOMIG-P2 is a Gram-negative γ -*Proteobacteria*. This strain is closely related to other *Proteobacteria* which degrade APAP including two strains of *Pseudomonas aeruginosa* isolated from membrane bioreactor (MBR) biomass (De Gusseme et al. 2011) and sequencing batch reactor (SBR) for treating APAP-contaminated wastewater (Hu et al. 2013), *Pseudomonas* sp. f2 and fg-2 isolated from SBR for treating APAP-contaminated wastewater (Zhang et al. 2013), *Stenotrophomonas* sp. f1 (Zhang et al., 2013), *Klebsiella pneumonia* S001 (Liang et al. 2016), and *Delftia tsuruhatensis* BDG1 (De Gusseme et al. 2011) (Figure 4.2).

The other species isolated from APAP degrading community included *Spingobium* sp. BIOMIG-P36 which is Gram-negative *Proteobacteria* and *Flavobacterium* sp. BIOMIG-P32 which belongs to *Bacteroidetes* phylum of *Bacteria* (Figure 4.2). Any APAP-degraders phylogenetically related to these species have not been reported in the literature to date; therefore these species are novel APAP-degraders identified in this study. Our results suggested that APAP-degraders are phylogenetically diverse and species from different genera and phyla of bacteria involve in APAP degradation in the environment.

4.3. APAP Biotransformation Kinetics of Four Isolates

Acetaminophen biotransformation kinetics assay by four isolates was performed the procedure described above. APAP was completely utilized within 40 hours in each flask (Figure 4.3). Estimated k' and K_{APAP} values were 3.86, 4.41, 4.21 and 6.38 mg/L.hr, and 10.48, 28.60, 38.40 and 49.27 mg/L for BIOMIG-P2, BIOMIG-P19, BIOMIG-P32, and BIOMIG-P36, respectively (Table 4.1). These results suggested that different species degrade acetaminophen at different rates. BIOMIG-P36 degraded APAP faster than the other strains tested. However, K_S was the major factor affecting the biotransformation rate which was above 10 mg/L for all the strains.

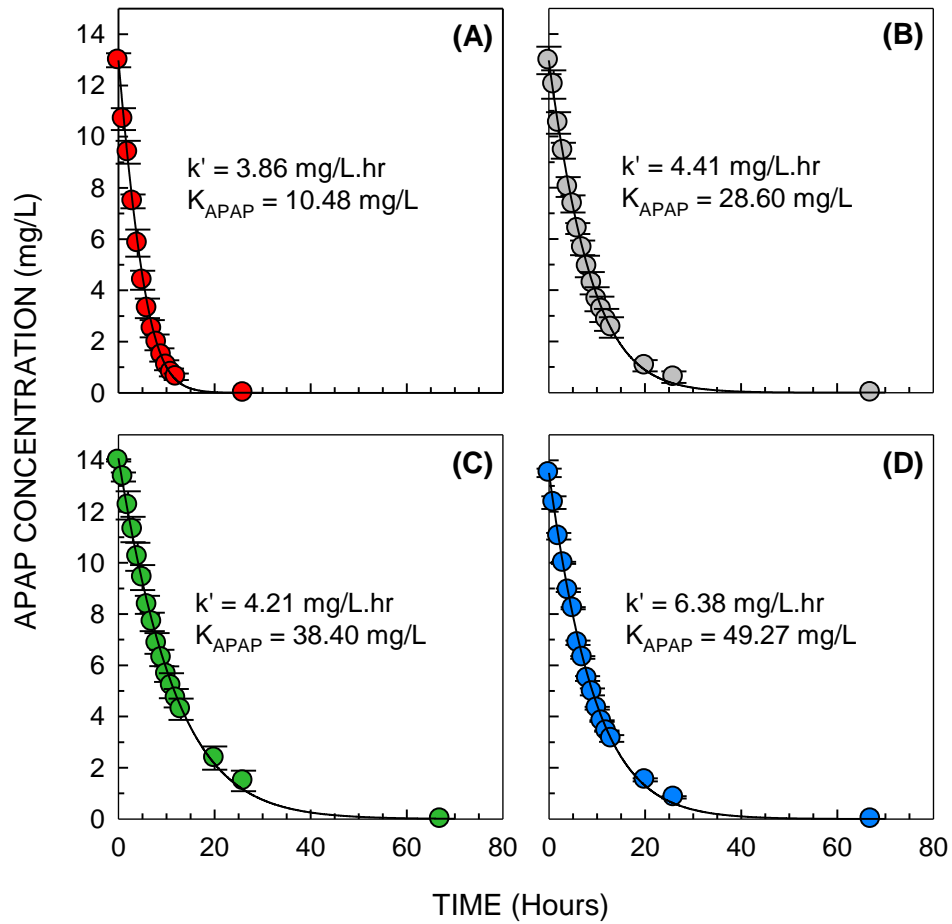


Figure 4.3. APAP utilization profiles by (A) *Pseudomonas nitroreducens* BIOMIG-P2, (B) *Rhodococcus erythropolis* BIOMIG-P19, (C) *Flavobacterium* sp. BIOMIG-P32, and (D) *Sphingobium* sp. BIOMIG-P36 at 10 mg/L concentration at 22°C (error bars represent one standard deviation of the mean, $n=3$)

Table 4.1. Biotransformation rate constants of BIOMIG-P isolates at 10 mg/L initial APAP concentration

| Rate Constants | Bacterial Strains | | | |
|-------------------|------------------------|------------------------|------------------------|------------------------|
| | BIOMIG-P2 | BIOMIG-P19 | BIOMIG-P32 | BIOMIG-P36 |
| K_{APAP} (mg/L) | 10.48 | 28.60 | 38.40 | 49.27 |
| k (mg/cells.hr) | 1.97×10^{-11} | 3.94×10^{-11} | 5.26×10^{-11} | 6.38×10^{-11} |
| k' (mg/L.hr) | 3.86 | 4.41 | 4.21 | 6.38 |

4.4. Growth Kinetics of BIOMIG-P19

Growth of BIOMIG-P19 in LB was monitored at temperatures between 5 and 45°C (Figure 4.4.A and H). Growth was not observed above 40°C (Figure 4.4.G and H). Growth was observed after 60 hours at 5°C (Figure 4.4.A). Specific growth rate and the corresponding doubling time at 5°C were 0.04 hr⁻¹ and 15.6 hr, respectively (Table 4.2). At 10°C, growth started after 20 hrs which was earlier than the growth at 5°C (Figure 4.4.B). The doubling time of BIOMIG-P19 at 10°C was the half of at 5°C. BIOMIG-P19 grew in LB broth with a rate of 0.13 hr⁻¹ which corresponds to a doubling time of 5.17 hr at 15°C (Figure 4.4.C). Specific growth rate and the doubling time at 22°C were 0.27 hr⁻¹ and 2.54 hr, respectively (Figure 4.4.D), almost twice as fast as the growth at 15°C. Doubling time of BIOMIG-P19 is comparable to that of *Bacillus subtilis* 168, and *Rhodococcus* sp. RHA1 which is equal to 0.43 and 5.3 hr, respectively (Bionumbers Database, 2016). Fastest growth was observed at 30°C (Figure 4.4.E). Lag phase was only 3.5 hours and exponential growth last for 11 hours. Growth was completed within 15 hours and growth rate was estimated as 0.36 hr⁻¹ with a doubling time of 1.93 hr. Moreover, doubling time of BIOMIG-P19 was 0.83 hr longer at 35°C than at 30°C (Table 4.2).

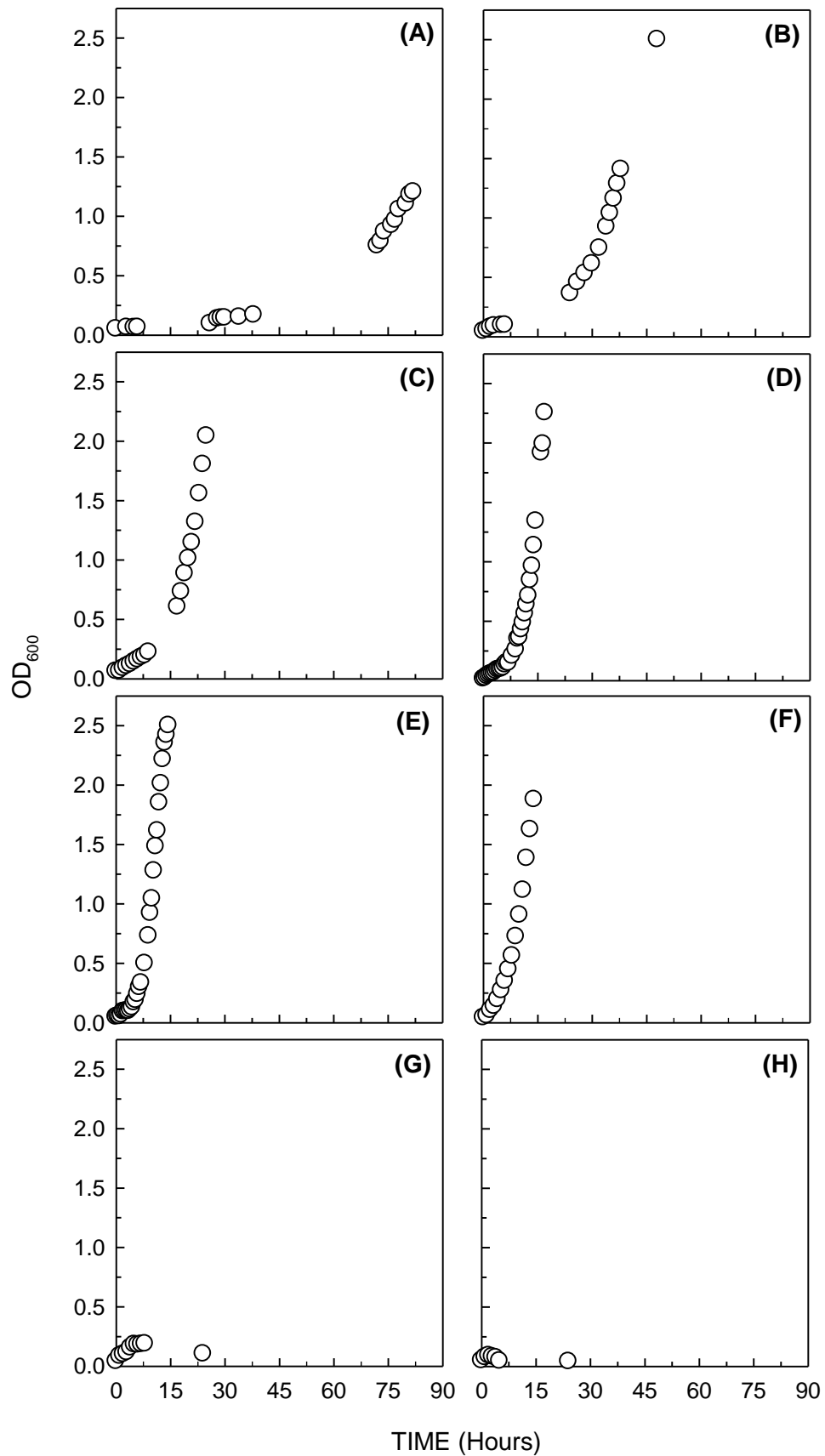


Figure 4.4. Growth profile of BIOMIG-P19 in LB broth at (A) 5°C, (B) 10°C, (C) 15°C, (D) 22°C, (E) 30°C, (F) 35°C, (G) 40°C and (H) 45°C

Table 4.2. Calculated specific growth rate and doubling time in LB broth at 5, 10, 15, 22, 30, 35 and 45°C

| Parameter | Temperature | | | | | | |
|--------------|-------------|------|------|------|------|------|------|
| | 5°C | 10°C | 15°C | 22°C | 30°C | 35°C | 45°C |
| μ (1/hr) | 0.04 | 0.10 | 0.13 | 0.27 | 0.36 | 0.25 | 0 |
| t_d (hr) | 15.6 | 7.22 | 5.17 | 2.54 | 1.93 | 2.76 | 0 |

Relationship between growth rate and temperature obeyed a modified Arrhenius model (Eqn. 4.1). As a result, optimum growth temperature of BIOMIG-P19 in LB broth was determined as 33°C (Figure 4.5). Optimum growth temperature of *Rhodococcus* sp. RHA1 which is a phlogenetically related strain to BIOMIG-P19 was stated as 30°C (Bionumbers Database, 2016).

$$\mu = \frac{\beta T \exp\left[\frac{-E_a}{RT}\right]}{1 + \exp\left[\frac{\Delta S}{R}\right] \exp\left[\frac{-\Delta H}{RT}\right]} \quad (4.1)$$

where; β is the biodegradation proportionality factor ($\mu\text{M/hr.K}$), T is the absolute temperature (K), E_a is the activation energy (kcal/mol), R is the ideal gas constant (1.987×10^{-3} kcal/mol.K), ΔS is the entropy change of enzyme deactivation (kcal/mol.K) and ΔH is the enthalpy change of enzyme deactivation (kcal/mol).

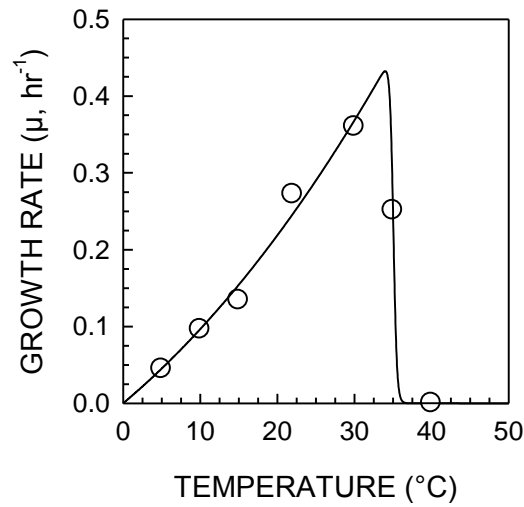


Figure 4.5. Relationship between temperature and growth rate

4.5. APAP Biotransformation by BIOMIG-P19

4.5.1. Effect of initial APAP concentration

APAP biotransformation kinetics assay evaluating the effect of initial APAP concentration was performed following the procedure described above by re-spiking the flasks at an initial APAP concentration of 1, 10, 100 and 500 mg/L. APAP was consumed within 24, 12, 6 and 10 hours in the flasks amended at 1, 10, 100 and 500 mg/L initial concentration, respectively (Fig. 4.6.A and B). APAP biotransformation rate was higher at high initial APAP concentrations compared to low concentrations. APAP biotransformation kinetics were simulated using Michaelis-Menten growth model (r^2 of fits >0.98) (Equation 4.2):

$$\frac{d[APAP]}{dt} = \frac{k [APAP] X}{K_{APAP} [APAP]} \quad (4.2)$$

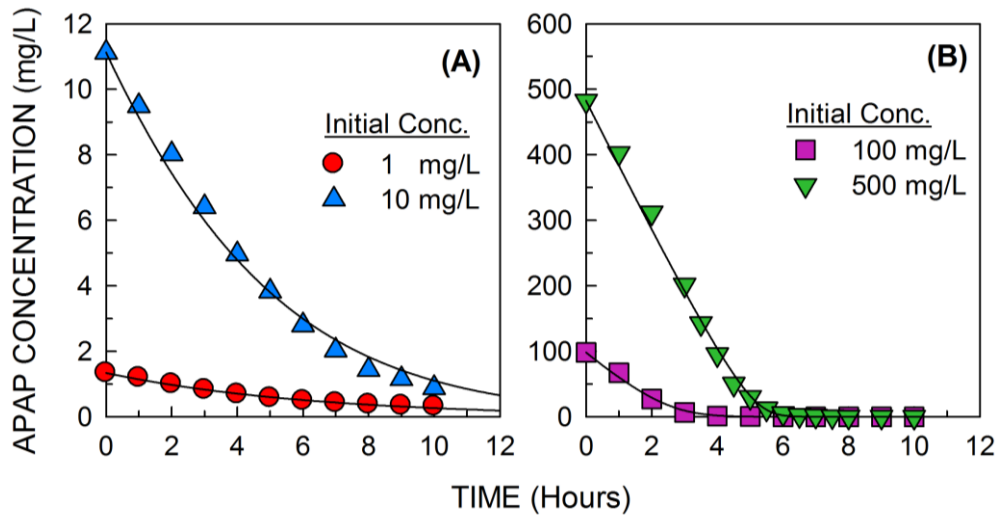


Figure 4.6. Profiles of APAP utilization by BIOMIG-P19 at (A) 1 and 10 mg/L and (B) 100 and 500 mg/L concentration at 22°C

Estimated k values for APAP at 1, 10, 100 and 500 mg/L initial concentration were 3.56×10^{-11} , 6.09×10^{-11} , 42.28×10^{-11} and 92.50×10^{-11} mg/cell.hr, respectively (Table 4.3). Obtained k values plotted against concentration and maximum k and K_{APAP} were estimated as $133 \pm 7 \times 10^{-11}$ mg/cell.h and 211 ± 28 mg/L ($r^2 = 0.99$), respectively (Figure 4.7). Similarly, Hu et al. (2013) reported observed rate constant (k') and K_{APAP} for *Pseudomonas aeruginosa* HJ1012 at 315 mg/L APAP concentration and 31.76 mg/L biomass concentration as 63.32 mg/L.h and 164.17 mg/L, respectively. High K_{APAP} values indicated that affinity of bacteria to APAP was low suggesting that biotransformation of this compound would be slow at environmentally relevant concentrations, which are below 1 mg/L. k' values for *Stenotrophomonas* sp. f1, *Pseudomonas* sp. f2 and *Pseudomonas* sp. fg-2 from the study of Zhang et al. (2013) were estimated as 98 mg/L.h, 330 mg/L.h and 405 mg/L.h, at APAP concentrations of 100 mg/L, 750 mg/L and 750 mg/L, respectively, which are comparable to the observed APAP degradation rate of BIOMIG-19.

Table 4.3. Biotransformation rate constants at APAP concentrations at 1, 10, 100 and 500 mg/L

| Rate Constants | Initial APAP Concentration (mg/L) | | | |
|------------------|-----------------------------------|------------------------|-------------------------|-------------------------|
| | 1 | 10 | 100 | 500 |
| k (mg/cell.hr) | 3.56×10^{-11} | 6.09×10^{-11} | 42.28×10^{-11} | 92.50×10^{-11} |
| k' (mg/L.hr) | 4.71 | 7.61 | 51.58 | 105.45 |

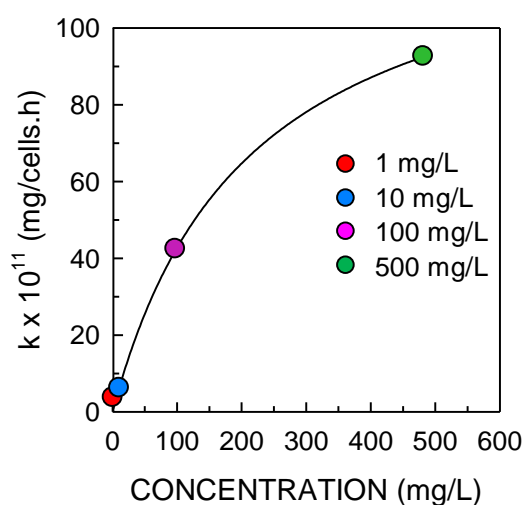


Figure 4.7. Cell specific biotransformation rate at APAP concentrations between 1 and 500 mg/L

4.5.2. Effect of initial cell density

Biotransformation of APAP by BIOMIG-P19 at different cell densities ranging from 10^9 to 10^{11} CFU/L was evaluated at 10 mg/L initial total APAP concentration. Biodegradation of APAP lasted about 100 h at 10^9 CFU/L. On the other hand, APAP was not utilized completely at this cell density, and APAP concentration stayed constant at 3.76 mg/L. At every cell density above 10^9 CFU/L, the biodegradation span decreased to 70, 50, 20 and 12 hr at 10^{10} , 2×10^{10} , 5×10^{10} and 10^{11} CFU/L, respectively (Figure 4.8). Although observed APAP degradation rates (k') linearly increased from 0.1 to 11.8 mg/L.hr between 10^9 and 10^{11} CFU/L, cell specific APAP utilization rate constant (k), which was $10.7 \pm 2.0 \times 10^{-11}$ mg/cell.hr, did not change (Figure 4.9). In addition, any lag-phase at cell densities above 10^9 CFU/L was not observed, degradation started immediately after APAP was introduced. Consequently, APAP biotransformation rate was decreased at lower cell

densities. Optimum cell density for efficient APAP biotransformation is about 10^{11} CFU/L, below this concentration rate of biotransformation decreases.

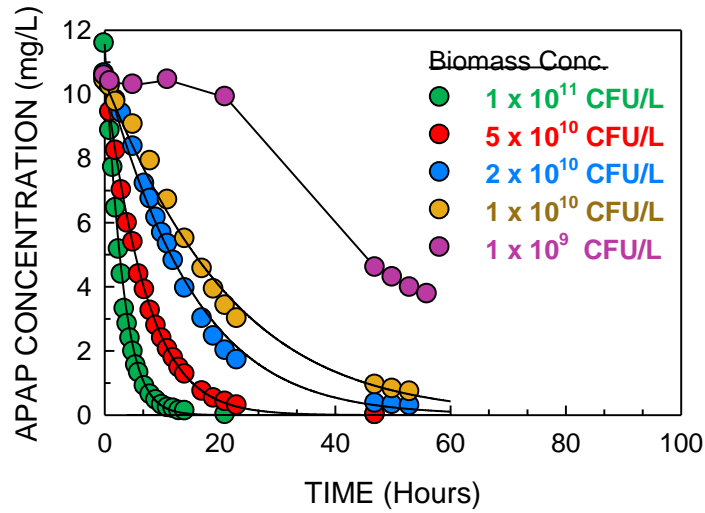


Figure 4.8. Profiles of APAP utilization by BIOMIG-P19 at 10 mg/L initial APAP concentration and different cell densities between 10^9 and 10^{11} CFU/L at 22°C

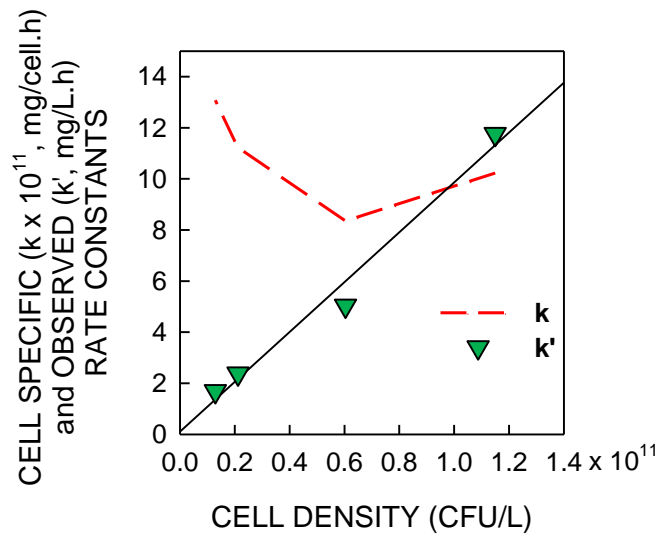


Figure 4.9. Profile of APAP biotransformation rates at cell densities between 10^{10} to 10^{11} CFU/L

4.5.3. Effect of temperature

APAP biotransformation by BIOMIG-P19 was monitored at temperatures 5, 10, 15, 22, 30, 35 and 45°C at 10 mg/L initial APAP concentration (Figures 4.10.A to H). Biotransformation of APAP was slow and lasted 40 h at 5°C (Figure 4.10.B). Duration of APAP biotransformation decreased to 30, 24 and 12 h at 10, 15, and above 22°C, respectively. The cell specific rate of APAP biotransformation doubled at every 10°C up to 22°C and was constant at $10.4 \pm 0.3 \times 10^{-11}$ mg/cell.hr between 22 and 35°C (Figure 4.11). APAP biotransformation was not observed at 45°C at which BIOMIG-P19 cannot grow even in LB broth. Only 28% of the APAP were degraded at 45°C (Figure 4.10.H). This evidence suggests that enzyme responsible for APAP biotransformation denatured after 2 hours following re-spiking with APAP.

Dependence of APAP biotransformation to temperature obeyed a modified Arrhenius equation (Equation 4) (Figure 4.11). The estimated parameters of relationship for APAP; $\beta = 5.06 \times 10^7$ $\mu\text{M}/\text{d.K}$; $E_a = 12.20$ kcal/mol; $\Delta S = 0.189$ kcal/mol.K; $\Delta H = 59.39$ kcal/mol. The optimum APAP biotransformation temperature was estimated as 28°C for BIOMIG-P19. Similarly, Hu et al. (2013) reported 30°C as the optimum APAP biotransformation temperature for *Pseudomonas aeruginosa* HJ1012.

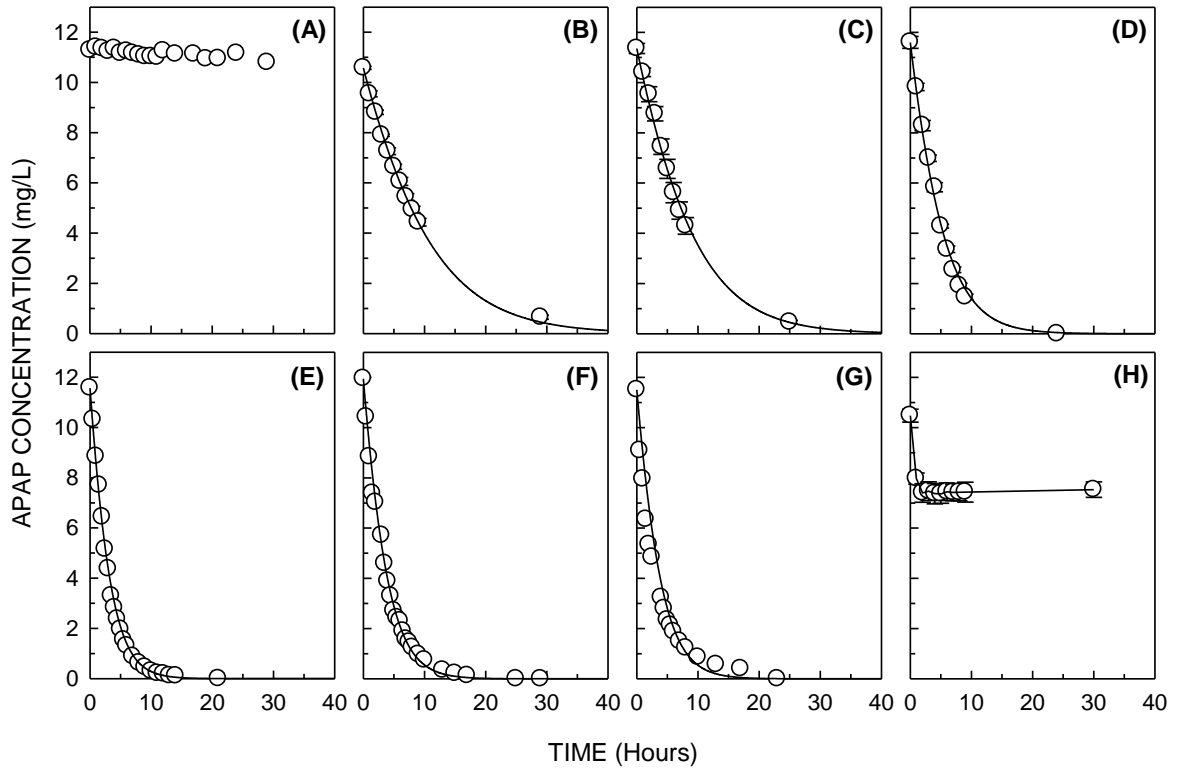


Figure 4.10. Profiles of APAP utilization by BIOMIG-P19 at (A) Control, (B) 5°C, (C) 10°C, (D) 15°C, (E) 22°C, (F) 30°C, (G) 35°C and (F) 45°C at 10 mg/L

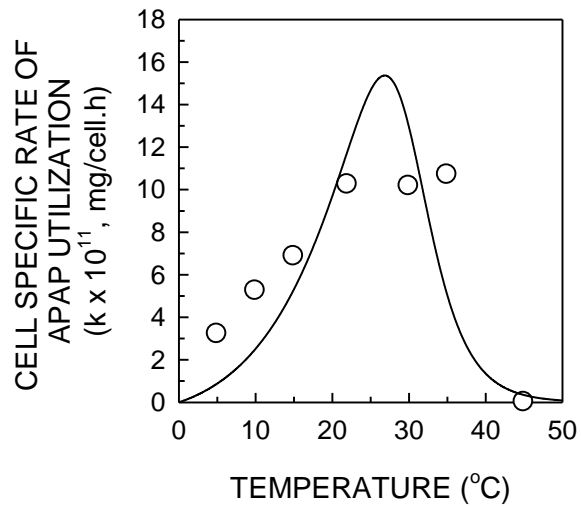


Figure 4.11. Profile of APAP biotransformation rate at 10 mg/L initial APAP concentration between 5 and 45°C

4.6. Threshold O₂ Concentration for APAP Biotransformation

In order to identify the threshold O₂ concentration and the preliminary pathway for APAP biodegradation, BIOMIG-P19 was introduced to 100 mg/L APAP in a closed serum bottle having limited amount of oxygen. As soon as APAP was introduced into the bottle, headspace O₂ started to decrease and accumulation of CO₂ was observed (Figure 4.12.A). After one day, headspace O₂ and CO₂ partial pressures were stabilized at 0.07 and 0.01 atm as soon as APAP was completely utilized (Figure 4.12).

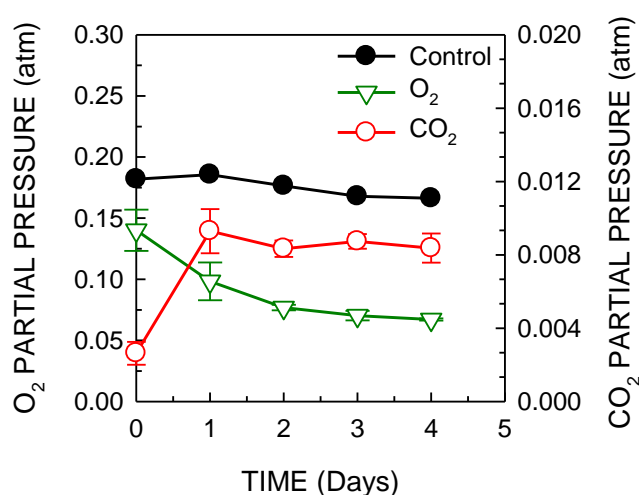


Figure 4.12. Profiles of headspace oxygen and carbon dioxide, spiked with 100 mg/L initial APAP concentration in control and test serum bottles inoculated with BIOMIG-P19

4.7. Determination of APAP Biotransformation Pathway

Kinetic experiments for metabolite analysis were performed in 250-mL Erlenmeyer flask. 4 mL of overnight grown culture of BIOMIG-P19 was transferred into 50 mL salt medium containing 100 mg/L initial APAP concentration to maintain c.a. 1×10^{11} CFU/L initial cell density in the flask. The flask was agitated on an orbital shaker at 130 rpm at 22°C room temperature. 1 mL of samples were taken from the flask, mixed with 1 mL of methanol with 2% formic acid, centrifuged at 10000 rpm for 10 min and then filtered through a 0.22- μ m filter at certain time intervals during the course of incubation. The control flask containing no microorganisms, and the reference flask containing microorganisms but no APAP were prepared exactly the same way described above and

monitored in the course of incubation. The samples which had been taken at appropriate time intervals were scanned in the EMS scan mode to acquire parent compounds distribution and change over time (Figure 4.14). In order to obtain a maximum of spectral information and increase confidence in compound identification, EPI spectra of the metabolites that have demonstrated increase and/or decrease trend in terms of their intensities compared within each other during the course of incubation were acquired and daughter ions were interpreted based upon the previous studies and literature (Figure 4.15, 4.16 and 4.17).

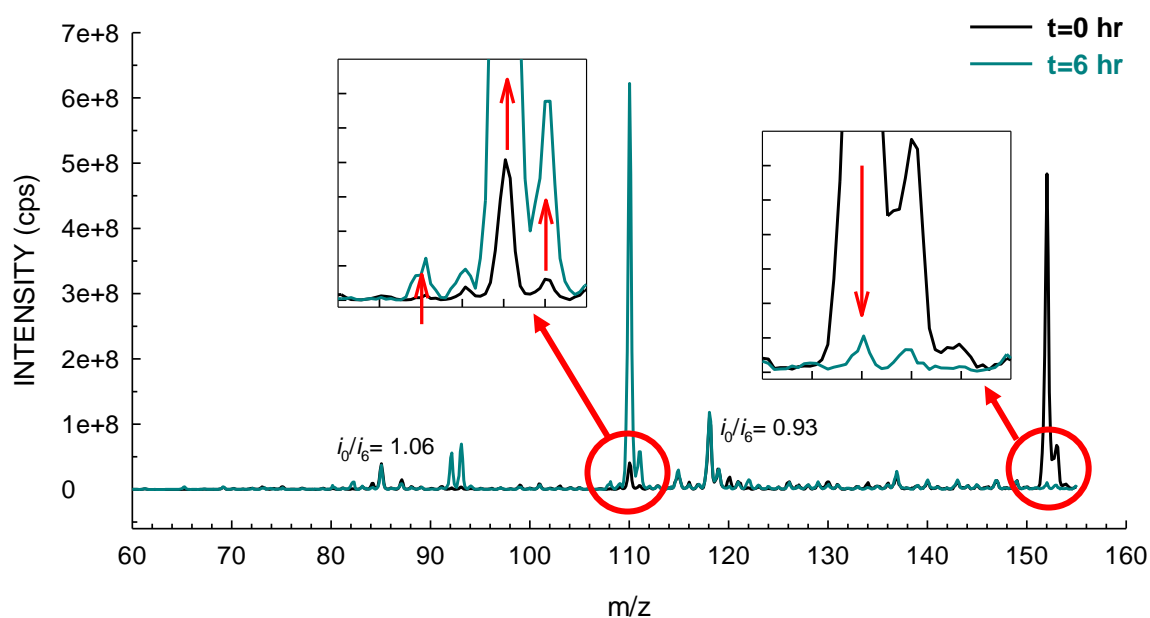


Figure 4.13. Overlaid EMS spectrum of samples taken at t=0 and t=6 hours showing the major parent compound distribution and change over time

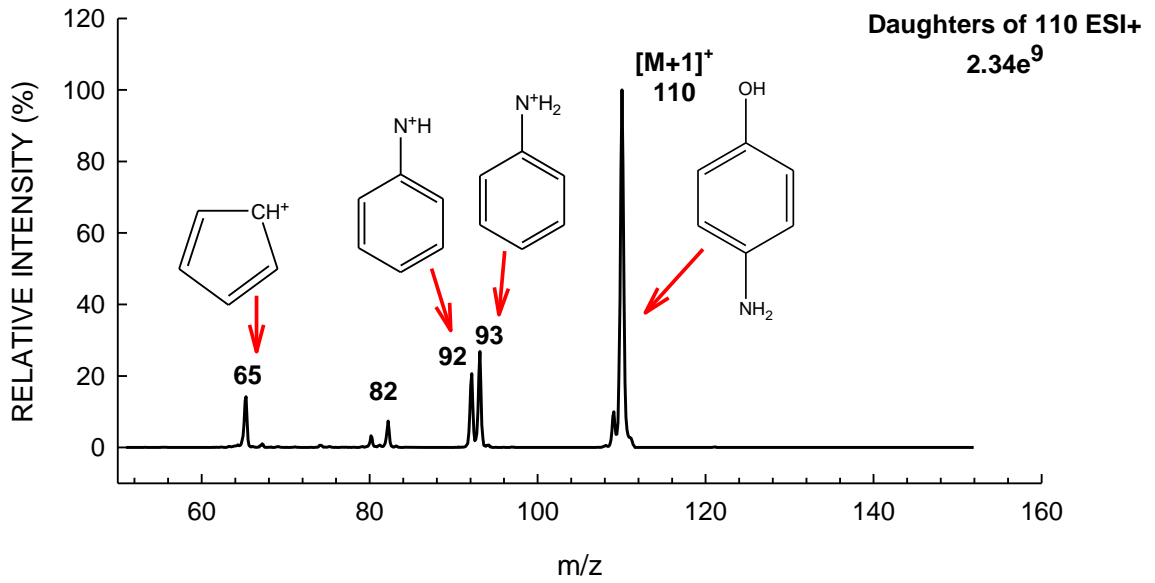


Figure 4.14. EPI spectrum of M1 with the proposed ion fragments. The molecular weight of M1 is 109. The m/z 110 corresponds to the $[M+H]^+$ parent ion

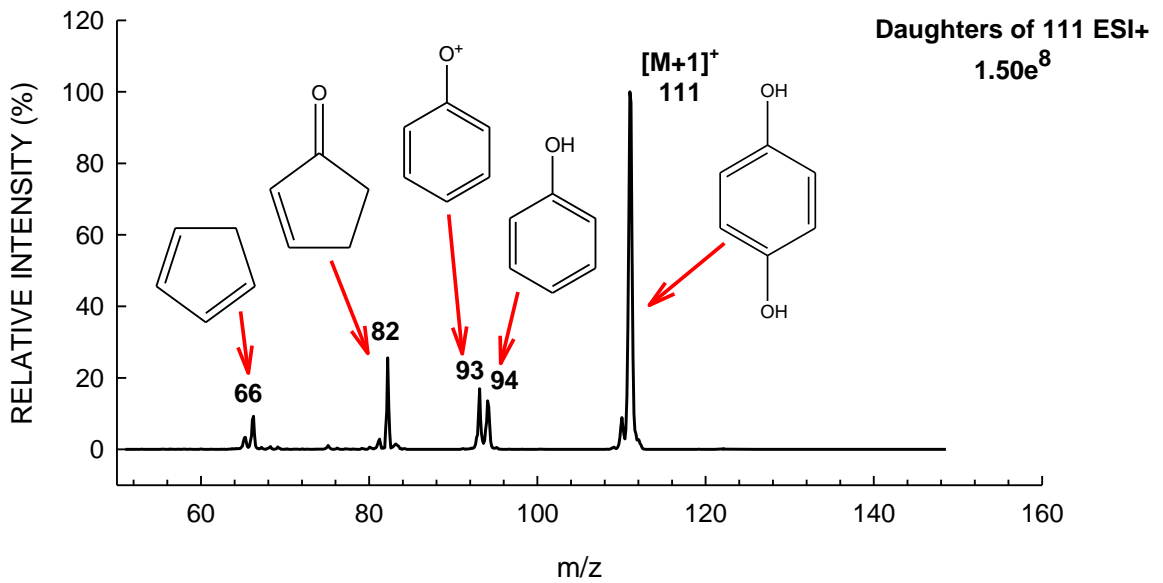


Figure 4.15. EPI spectrum of M2 with the proposed ion fragments. The molecular weight of M2 is 110. The m/z 111 corresponds to the $[M+H]^+$ parent ion

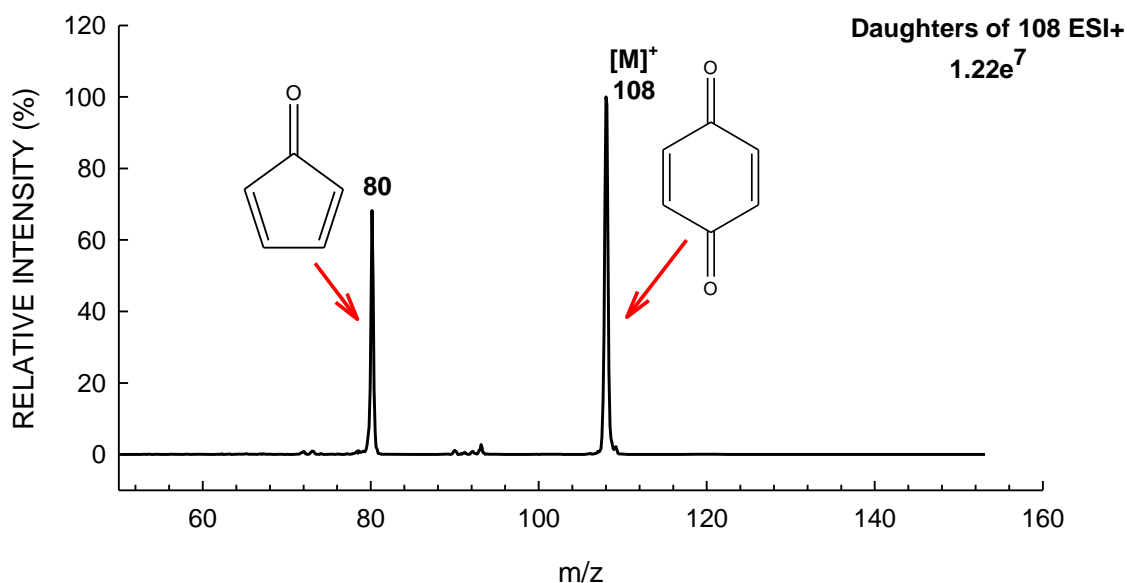


Figure 4.16. EPI spectrum of M3 with the proposed ion fragments. The molecular weight of M3 is 108. The m/z 108 corresponds to the $[M]^+$ parent ion

During APAP biotransformation, 3 by-products were detected with MS/MS over the m/z range from 55 to 155. M1, M2 and M3 were the most abundant by-products formed as APAP was degraded and utilized within 4 days (Figure 4.18). As M1 started to getting utilized, M2 and M3 accumulated in the bottle. Based on the information in the literature, HMDB Database and comparison of by-product spectra with the spectra of standard chemicals, M1, M2, and M3 were assigned as *p*-aminophenol, hydroquinone and 1,4-benzoquinone. Based on these observations, APAP was initially converted to *p*-aminophenol which was then transformed to hydroquinone by substitution of amino group with hydroxyl. Hydroquinone then goes into ring fusion and transformed to 1,4-benzoquinone which was responsible of brown-red coloration during biotransformation (Figure 4.19). In addition, Zhang et al. (2013) suggested that hydroxylation of APAP could potentially be catalyzed by a hydrolytic enzyme to produce hydroquinone with a release of acetamide, which could be further converted to 1,4-benzoquinone and an organic acid.

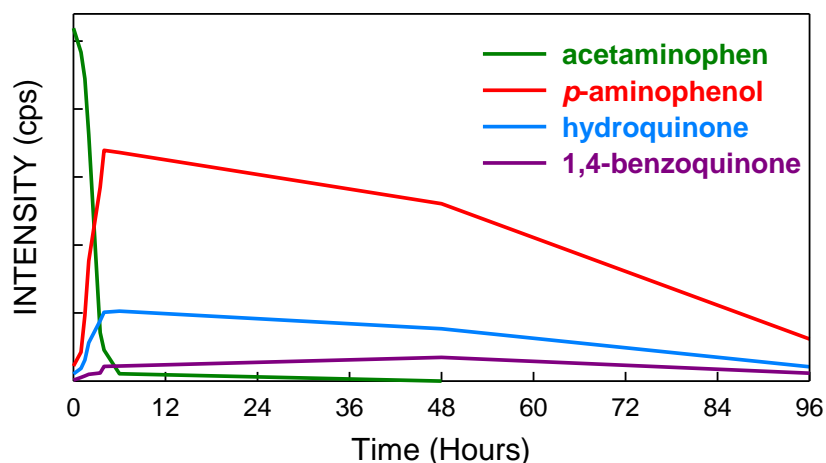


Figure 4.17. APAP and its biotransformation by-products inoculated with BIOMIG-P19

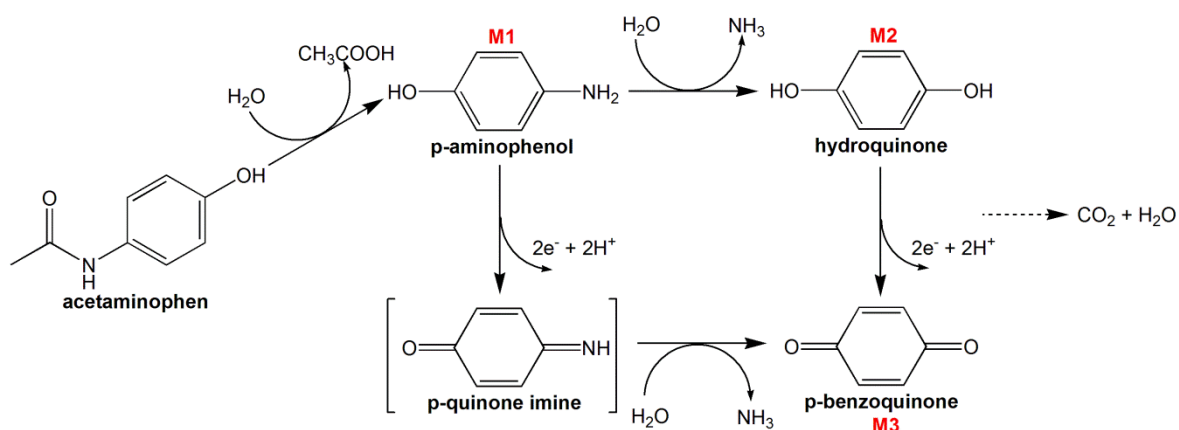


Figure 4.18. Proposed pathway of APAP biotransformation by BIOMIG-P19

4.8. Enzyme Kinetics of BIOMIG-P cells

The crude protein extracts of uninduced and induced APAP degraders were compared. Each extract contained proteins with a size primarily between 30-75 kDa (Figure 4.20). We have not identified a certain protein band which is common in induced APAP-degrader extracts and missing in uninduced cell extracts which may be the enzyme that transforms APAP.

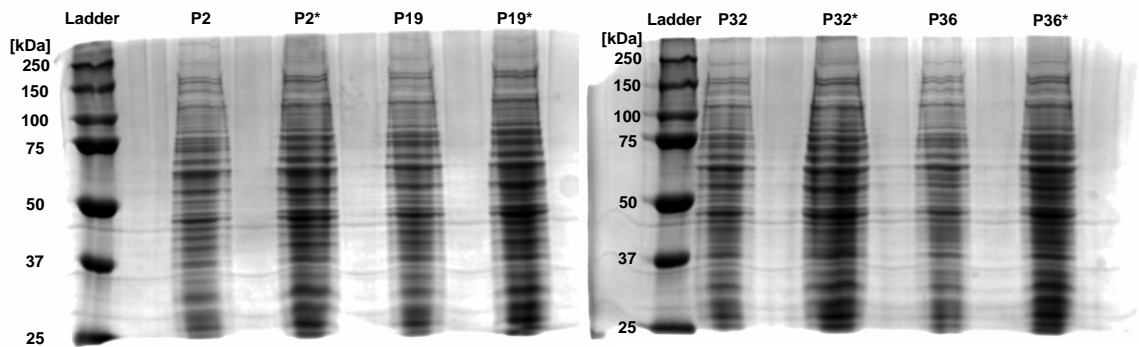


Figure 4.19. SDS-PAGE with protein ladder standard Precision Plus Protein™ Dual Xtra from Bio-Rad. Comparison of crude protein between BIOMIG-P2, BIOMIG-P19, BIOMIG-P32 and BIOMIG-P36. (*: Indicates the cells induced with acetaminophen prior to cell disruption)

APAP biotransformation by crude enzymes of BIOMIG-P cells at 10 mg/L initial APAP concentration was monitored for 45 hours. Enzyme concentrations in reactors were 0.58, 0.35, 0.31 and 0.58 mg/mL for P2, P19, P32 and P36, respectively. BIOMIG-P2 enzymes degraded APAP at a faster rate than the other enzymes. On the other hand, APAP was not utilized completely in all reactors during the course of experiment. Biodegradation extent of APAP in the reactors containing enzymes of BIOMIG-P2; BIOMIG-P19, BIOMIG-P32 and BIOMIG-P36 were approximately 96, 89, 60 and 87%, respectively (Figures 4.21.A to D). Additionally, there was 15 hours of lag phase prior to degradation in the reactor containing BIOMIG-P36 enzymes.

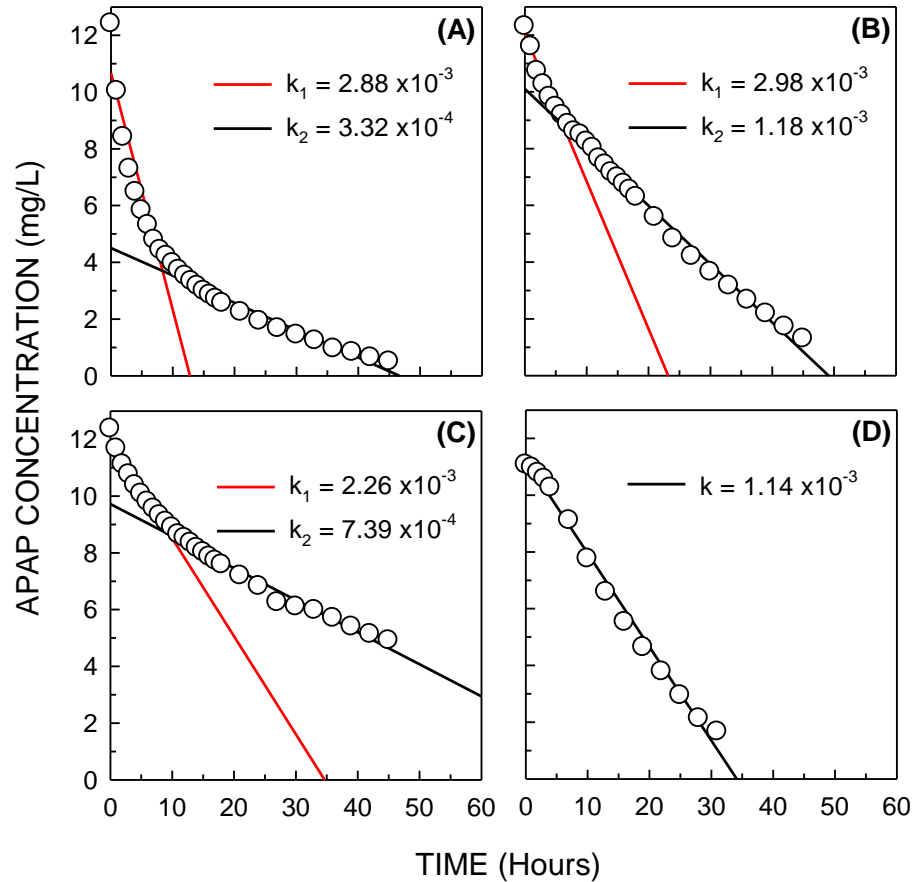


Figure 4.20. Profiles of APAP utilization by Enzymes of (A) BIOMIG-P2, (B) BIOMIG-P19, (C) BIOMIG-P32 and (D) BIOMIG-P36 cells at 10 mg/L initial APAP concentration (k : mg APAP/mg protein.hour)

4.9. APAP Biotransformation Kinetics of Enzyme Beads

Biodegradation of APAP by immobilized enzymes of BIOMIG-P19 was evaluated in 250 mL Erlenmeyer flasks containing c.a. 1.5 mg protein and 10 mg/L APAP concentration. The concentration of APAP in the control reactor did not change. During the first 6 hours of experiment, APAP concentration decreased approximately 3 mg/L with a linear trend, and then the following 4 days the rate of change in APAP concentration decreased sharply. At 5th day, increase in the rate of change in APAP concentration was observed and APAP was utilized completely at 12th day (Figure 4.22).

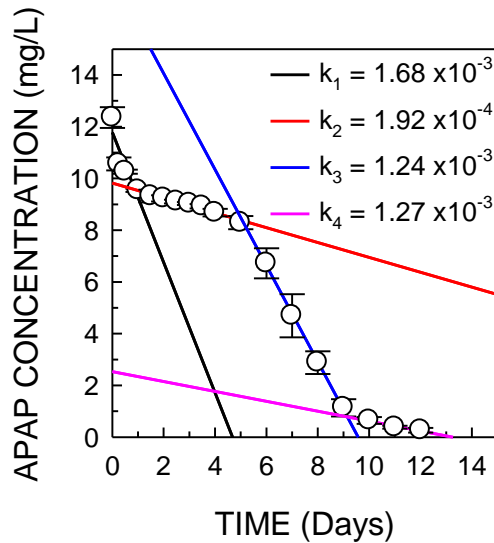


Figure 4.21. Profiles of APAP utilization by immobilized enzymes of BIOMIG-P19
(k: mg APAP/mg protein.days)

The mechanisms initiating APAP biotransformation by immobilized enzymes can be explained by adsorption and diffusional limitations. At first 6 hour time span, adsorption of APAP molecules on enzyme beads may be the responsible mechanism for the change in substrate concentration (Figure 4.23). After this point, biodegradation may take place with a slow rate due to diffusion of APAP molecules in enzyme beads. Furthermore, the rate of APAP diffusion may be slower than the rate of its biotransformation; resulting in a decrease in contact of all APAP molecules with the immobilized enzymes entrapped in Calcium alginate beads.

In addition, Na-alginate concentration may cause a decrease in diffusion ability of APAP into the beads. Since increasing the concentration of Na-alginate solution results in tightly cross-linked beads decreasing the pore size of the beads (Mahajan et al. 2010). CaCl_2 concentration, which retains the stability of beads, may also affect the enzyme activity. Furthermore, low enzyme concentration in the beads and large bead diameter may affect the enzyme activity negatively.

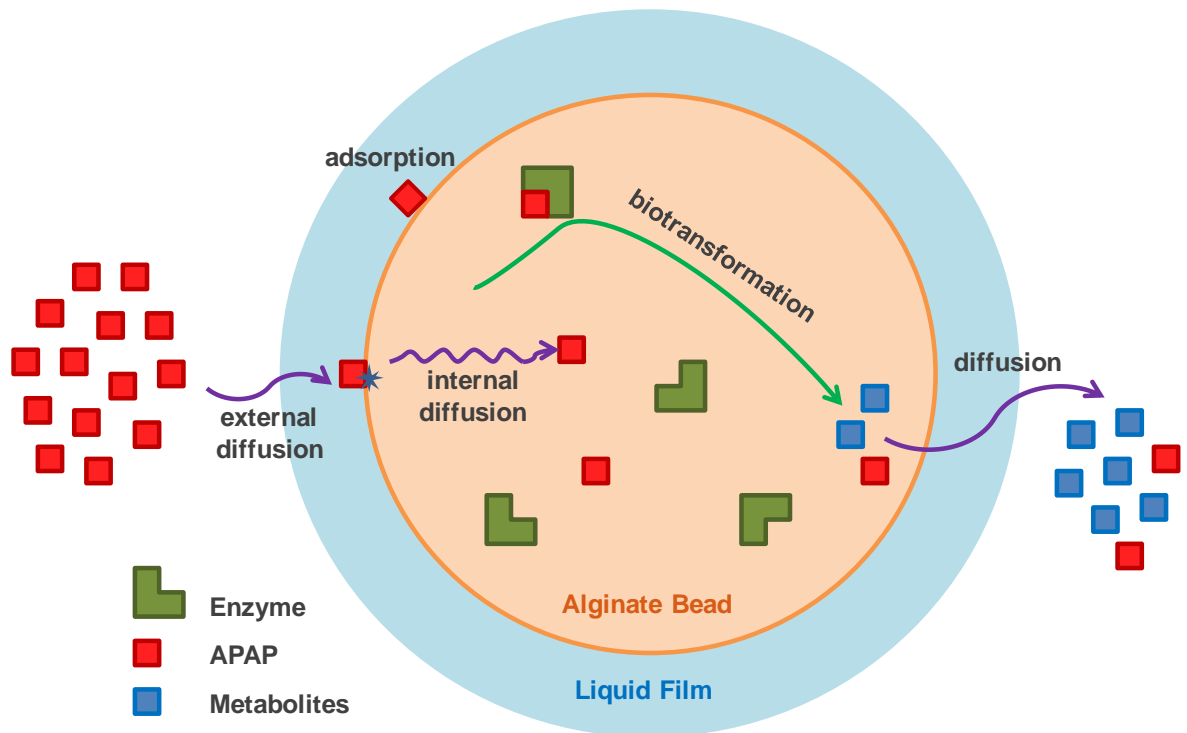


Figure 4.22. Proposed mechanisms initiating APAP biotransformation by immobilized enzymes

5. CONCLUSIONS

In this research, four phylogenetically distinct bacteria, which are capable of degrading APAP, were isolated from soil microbial community. Most abundant species in the community was identified as *Rhodococcus erythropolis* BIOMIG-P19, which is a Gram-positive *Actinobacteria* well-known with their ability to utilize aromatic compounds. Any APAP-degraders phylogenetically related to *Sphingobium* sp. BIOMIG-P36 and *Flavobacterium* sp. BIOMIG-P32 have not been reported in the literature to date; therefore these species are novel APAP-degraders identified based on their 16S rRNA gene with an average nucleotide identity (ANI) below 97% via phylogenetic analysis. Only the bacteria *Pseudomonas nitroreducens* BIOMIG-P2 is closely related to the bacteria reported in the literature. Those findings suggest that APAP-degraders are phylogenetically diverse and species from different genera and phyla of bacteria involve in APAP degradation in the environment.

APAP biodegradation by *Rhodococcus erythropolis* BIOMIG-P19 follows Michaelis-Menten kinetics with a maximum cell specific APAP utilization rate and maximum half-saturation constant of $133 \pm 7 \times 10^{-11}$ mg/cell.h and of 211 ± 28 mg/L, respectively. Additionally, APAP biotransformation rate decreases as initial APAP concentration decreases. APAP biotransformation is also affected by cell density especially below a density of 5×10^{10} CFU/L, APAP utilization rate decreases. Maximum rate of APAP degradation was achieved at temperature range between 22 and 35°C while optimum temperature is at 28 °C. The main metabolite during APAP biodegradation was identified as *p*-aminophenol which then was converted to hydroquinone and 1,4-benzoquinone by a series of oxidation and hydroxylation reactions. Due to very high half-saturation constant, its biotransformation in the environment is very slow at environmentally relevant concentrations, which may justify why APAP is frequently detected in the environment at concentrations below mg/L. In addition, APAP utilization by immobilized enzymes lasted 12 days at 10 mg/L initial APAP. As a result, removal of APAP in wastewater and soil especially at concentrations below mg/L is very difficult by both using microorganisms and their immobilized enzymes; therefore innovative technologies are needed for treatment.

REFERENCES

Albero, B., Sanchez-Brunete, C., Miguel, E., Aznar, R., Tadeo, J.L., 2014. Determination of selected pharmaceutical compounds in biosolids by supported liquid extraction and gas chromatography-tandem mass spectrometry. *Journal of Chromatography A*, 1336, 52-58.

ANSES (2011). Campagne nationale d'occurrence des résidus de médicaments dans les eaux destinées à la consommation humaine.

<http://www.anses.fr/sites/default/files/documents/LABO-RaEtudeMedicamentsEaux.pdf>

Antunes, S.C., Freitas, R., Figueira, E., Gonçalves, F., Nunes, B., 2013. Biochemical effects of acetaminophen in aquatic species: edible clams *Venerupis decussata* and *Venerupis philippinarum*. *Environmental Science and Pollution Research*, 20, 6658-6666.

Aravindhan, R., 2014. Kinetics of biodegradation of phenol and a polyphenolic compound by a mixed culture containing *Pseudomonas aeruginosa* and *Bacillus subtilis*. *Applied Ecology and Environmental Research*, 12, 615-625.

Ba, S., Haroune, L., Cruz-Morato, C., Jacquet, C., Touahar, I.E., Bellenger, J.P., Legault, C.Y., Jones, J.P., Cabana, H., 2014. Synthesis and characterization of combined cross-linked laccase and tyrosinase aggregates transforming acetaminophen as a model phenolic compound in wastewaters. *Science of the Total Environment*, 487, 748-755.

Barra Caracciolo, A., Topp, E., Grenni, P., 2015. Pharmaceuticals in the environment: biodegradation and effects on natural microbial communities. A review. *Journal of Pharmaceutical and Biomedical Analysis*, 106, 25-36.

Bartha, B., Huber, C., Harpaintner, R., Schroder, P., 2010. Effects of acetaminophen in *Brassica juncea* L. Czern.: investigation of uptake, translocation, detoxification, and the induced defense pathways. *Environmental Science and Pollution Research*, 17, 1553-1562.

Bedner, M., MacCrehan, W.A., 2006. Transformation of acetaminophen by chlorination produces the toxicants 1,4-benzoquinone and N-acetyl-p-benzoquinone imine. *Environmental Science and Technology*, 40, 516-522.

Berling, I., Anscombe, M., Isbister, G.K., 2011. Intravenous paracetamol toxicity in a malnourished child. *Clinical Toxicology*, 50, 74-76.

Bickerstaff, G.F., 1997. Immobilization of enzymes and cells. Bickerstaff, G.F. (ed.), Humana Press, Totowa, NJ, 1-11.

Bionumbers Database, 2016.

<http://bionumbers.hms.harvard.edu/> (accessed June 17, 2016).

Bio-Rad Bulletin 6040 Rev B. A guide to polyacrylamide gel electrophoresis and detection.

http://www.bio-rad.com/webroot/web/pdf/lsr/literature/Bulletin_6040.pdf

Boleda, M.R., Galceran, M.T., Ventura, F., 2011. Behavior of pharmaceuticals and drugs of abuse in a drinking water treatment plant (DWTP) using combined conventional and ultrafiltration and reverse osmosis (UF/RO) treatments. *Environmental Pollution*, 159, 1584-1591.

Bouissou-Schurtz, C., Houeto, P., Guerbet, M., Bachelot, M., Casellas, C., Mauclair, A.C., Panetier, P., Delval, C., Masset, D., 2014. Ecological risk assessment of the presence of pharmaceutical residues in a French national water survey. *Regulatory Toxicology and Pharmacology*, 69, 296-303.

Brandão, F.P., Pereira, J.L., Gonçalves, F., Nunes, B., 2014. The impact of paracetamol on selected biomarkers of the mollusc species *Corbicula fluminea*. *Environmental Toxicology*, 29, 74-83.

Chen, C.Y., Chen, S.C., Fingas, M., Kao, C.M., 2010. Biodegradation of propionitrile by *Klebsiella oxytoca* immobilized in alginate and cellulose triacetate gel. *Journal of*

Hazardous Materials, 177, 856-863.

Chonova, T., Keck, F., Labanowski, J., Montuelle, B., Rimet, F., Bouchez, A., 2016. Separate treatment of hospital and urban wastewaters: A real scale comparison of effluents and their effect on microbial communities. *Science of the Total Environment*, 542, 965-975.

Clara, M., Strenn, B., Gans, O., Martinez, E., Kreuzinger, N., Kroiss, H., 2005. Removal of selected pharmaceuticals, fragrances and endocrine disrupting compounds in a membrane bioreactor and conventional wastewater treatment plants. *Water Research*, 39, 4797-4807.

Conley, J.M., Symes, S.J., Schorr, M.S., Richards, S.M., 2008. Spatial and temporal analysis of pharmaceutical concentrations in the upper Tennessee River basin. *Chemosphere*, 73, 1178-1187.

Correia, B., Freitas, R., Figueira, E., Soares, A.M., Nunes, B., 2016. Oxidative effects of the pharmaceutical drug paracetamol on the edible clam *Ruditapes philippinarum* under different salinities. *Comparative Biochemistry and Physiology C: Toxicology and Pharmacology*, 179, 116-124.

Dalgic, G., 2013. Parasetamol Iceren Atiklarda Kirletici Parametrelerin Gideriminde Ileri Oksidasyon Yontemlerinin Uygulanmasi, M.S. Thesis, Yildiz Technical University.

De Gusseme, B., Vanhaecke, L., Verstraete, W., Boon, N., 2011 Degradation of acetaminophen by *Delftia tsuruhatensis* and *Pseudomonas aeruginosa* in a membrane bioreactor. *Water Research*, 45, 1829-1837.

de Wilt, A., Butkovskiy, A., Tuantet, K., Leal, L.H., Fernandes, T.V., Langenhoff, A., Zeeman, G., 2016. Micropollutant removal in an algal treatment system fed with source separated wastewater streams. *Journal of Hazardous Materials*, 304, 84-92.

Escapa, C., Coimbra, R.N., Paniagua, S., Garcia, A.I., Otero, M., 2015. Nutrients and pharmaceuticals removal from wastewater by culture and harvesting of *Chlorella*

sorokiniana. *Bioresource Technology*, 185, 276-284.

Farré, M.I., Pérez, S., Kantiani, L., Barceló, D., 2008. Fate and toxicity of emerging pollutants, their metabolites and transformation products in the aquatic environment. *TrAC Trends in Analytical Chemistry*, 27, 991-1007.

Fent, K., Weston, A.A., Caminada, D., 2006. Ecotoxicology of human pharmaceuticals. *Aquatic Toxicology*, 76, 122-159.

Fram, M.S., Belitz, K., 2011. Occurrence and concentrations of pharmaceutical compounds in groundwater used for public drinking-water supply in California. *Science of the Total Environment*, 409, 3409-3417.

Galus, M., Jeyaranjan, J., Smith, E., Li, H., Metcalfe, C., Wilson, J.Y., 2013a. Chronic effects of exposure to a pharmaceutical mixture and municipal wastewater in zebrafish. *Aquatic Toxicology*, 132-133, 212-222.

Galus, M., Kirischian, N., Higgins, S., Purdy, J., Chow, J., Ranganjan, S., Li, H., Metcalfe, C., Wilson, J.Y., 2013b. Chronic, low concentration exposure to pharmaceuticals impacts multiple organ systems in zebrafish. *Aquatic Toxicology*, 132-133, 200-211.

Georgieva, S., Godjevargova, T., Mita, D.G., Diano, N., Menale, C., Nicolucci, C., Carratelli, C.R., Mita, L., Golovinsky, E., 2010. Non-isothermal bioremediation of waters polluted by phenol and some of its derivatives by laccase covalently immobilized on polypropylene membranes. *Journal of Molecular Catalysis B: Enzymatic*, 66, 210-218.

Glassmeyer, S.T., Shoemaker, J.A., 2005. Effects of Chlorination on the Persistence of Pharmaceuticals in the Environment. *Bulletin of Environmental Contamination and Toxicology*, 74, 24-31.

Gomez, M.J., Martinez Bueno, M.J., Lacorte, S., Fernandez-Alba, A.R., Aguera, A., 2007. Pilot survey monitoring pharmaceuticals and related compounds in a sewage treatment plant located on the Mediterranean coast. *Chemosphere*, 66, 993-1002.

Gómez-Oliván, L.M., Neri-Cruz, N., Galar-Martínez, M., Vieyra-Reyes, P., García-Medina, S., Razo-Estrada, C., Dublán-García, O., Corral-Avitia, A.Y., 2012. Assessing the Oxidative Stress Induced by Paracetamol Spiked in Artificial Sediment on *Hyalella azteca*. *Water, Air and Soil Pollution*, 223, 5097-5104.

Gros, M., Petrovic, M., Barcelo, D., 2006. Development of a multi-residue analytical methodology based on liquid chromatography-tandem mass spectrometry (LC-MS/MS) for screening and trace level determination of pharmaceuticals in surface and wastewaters. *Talanta*, 70, 678-690.

Gros, M., Rodríguez-Mozaz, S., Barceló, D., 2012. Fast and comprehensive multi-residue analysis of a broad range of human and veterinary pharmaceuticals and some of their metabolites in surface and treated waters by ultra-high-performance liquid chromatography coupled to quadrupole-linear ion trap tandem mass spectrometry. *Journal of Chromatography A*, 1248, 104-121.

Grujic, S., Vasiljevic, T., Lausevic, M., 2009. Determination of multiple pharmaceutical classes in surface and ground waters by liquid chromatography-ion trap-tandem mass spectrometry. *Journal of Chromatography A*, 1216, 4989-5000.

Hart, A., Orr, D.L., 1975. The degradation of paracetamol (4-hydroxyacetanilide) and other substituted acetanilides by a *Penicillium* species. *Antonie Van Leeuwenhoek*, 41, 239-247.

Heberer, T., 2002. Occurrence, fate, and removal of pharmaceutical residues in the aquatic environment: a review of recent research data. *Toxicology Letters*, 131, 5-17.

Hinson, J.A., Reid, A.B., McCullough, S.S., James, L.P., 2004. Acetaminophen-induced hepatotoxicity: role of metabolic activation, reactive oxygen/nitrogen species, and mitochondrial permeability transition. *Drug Metabolism Reviews*, 36, 805-822.

Hu, J., Zhang, L.L., Chen, J.M., Liu, Y., 2013. Degradation of paracetamol by *Pseudomonas aeruginosa* strain HJ1012. *Journal of Environmental Science and Health A:*

Toxic/Hazardous Substances and Environmental Engineering, 48, 791-799.

Huber, M.M., Gobel, A., Joss, A., Hermann, N., Loffler, D., McArdell, C.S., Ried, A., Siegrist, H., Ternes, T.A., von Gunten, U., 2005. Oxidation of pharmaceuticals during ozonation of municipal wastewater effluents: a pilot study. *Environmental Science and Technology*, 39, 4290-4299.

Husain, Q., Ulber, R., 2011. Immobilized Peroxidase as a Valuable Tool in the Remediation of Aromatic Pollutants and Xenobiotic Compounds: A Review. *Critical Reviews in Environmental Science and Technology*, 41, 770-804.

Ivshina, I.B., Rychkova, M.I., Vikhareva, E.V., Chekryshkina, L.A., Mishenina, I.I., 2006. Catalysis of the biodegradation of unusable medicines by Alkanotrophic rhodococci. *Applied Biochemistry and Microbiology*, 42, 392-395.

Johnston, J.J., Savarie, P.J., Primus, T.M., Eisemann, J.D., Hurley, J.C., Kohler, D.J., 2002. Risk assessment of an acetaminophen baiting program for chemical control of brown tree snakes on Guam: evaluation of baits, snake residues, and potential primary and secondary hazards. *Environmental Science and Technology*, 36, 3827-3833.

Joss, A., Zabczynski, S., Gobel, A., Hoffmann, B., Loffler, D., McArdell, C.S., Ternes, T.A., Thomsen, A., Siegrist, H., 2006. Biological degradation of pharmaceuticals in municipal wastewater treatment: proposing a classification scheme. *Water Research*, 40, 1686-1696.

Kadakol, J.C., Kamanavalli, C.M., Shouche, Y., 2010. Biodegradation of Carbofuran phenol by free and immobilized cells of *Klebsiella pneumoniae* ATCC13883T. *World Journal of Microbiology and Biotechnology*, 27, 25-29.

Khetan, S.K., Collins, T.J., 2007. Human pharmaceuticals in the aquatic environment: a challenge to Green Chemistry. *Chemical Reviews*, 107, 2319-2364.

Kim, P., Park, Y., Ji, K., Seo, J., Lee, S., Choi, K., Kho, Y., Park, J., Choi, K., 2012. Effect

of chronic exposure to acetaminophen and lincomycin on Japanese medaka (*Oryzias latipes*) and freshwater cladocerans *Daphnia magna* and *Moina macrocopa*, and potential mechanisms of endocrine disruption. *Chemosphere*, 89, 10-18.

Kim, S.D., Cho, J., Kim, I.S., Vanderford, B.J., Snyder, S.A., 2007. Occurrence and removal of pharmaceuticals and endocrine disruptors in South Korean surface, drinking, and waste waters. *Water Research*, 41, 1013-1021.

Kolpin, D.W., Furlong, E.T., Meyer, M.T., Thurman, E.M., Zaugg, S.D., Barber, L.B., Buxton, H.T., 2002. Pharmaceuticals, hormones, and other organic wastewater contaminants in U.S. streams, 1999-2000: a national reconnaissance. *Environmental Science and Technology*, 36, 1202-1211.

Komesli, O.T., Muz, M., Ak, M.S., Bakirdere, S., Gokcay, C.F., 2015. Occurrence, fate and removal of endocrine disrupting compounds (EDCs) in Turkish wastewater treatment plants. *Chemical Engineering Journal*, 277, 202-208.

Kosma, C.I., Lambropoulou, D.A., Albanis, T.A., 2014. Investigation of PPCPs in wastewater treatment plants in Greece: Occurrence, removal and environmental risk assessment. *Science of the Total Environment*, 466-467, 421-438.

Kummerova, M., Zezulka, S., Babula, P., Triska, J., 2016. Possible ecological risk of two pharmaceuticals diclofenac and paracetamol demonstrated on a model plant *Lemna minor*. *Journal of Hazardous Materials*, 302, 351-361.

Lam, M.W., Young, C.J., Brain, R.A., Johnson, D.J., Hanson, M.A., Wilson, C.J., Richards, S.M., Solomon, K.R., Mabury, S.A., 2004. Aquatic persistence of eight pharmaceuticals in a microcosm study. *Environmental Toxicology and Chemistry*, 23, 1431-1440.

Li, J., Ye, Q., Gan, J., 2014. Degradation and transformation products of acetaminophen in soil. *Water Research*, 49, 44-52.

Li, T., Liu, J., Bai, R., Ohandja, D.G., Wong, F.S., 2007. Biodegradation of organonitriles by adapted activated sludge consortium with acetonitrile-degrading microorganisms. *Water Research*, 41, 3465-3473.

Liang, C., Lan, Z., Zhang, X., Liu, Y., 2016. Mechanism for the primary transformation of acetaminophen in a soil/water system. *Water Research*, 98, 215-224.

Lin, A.Y., Lin, C.A., Tung, H.H., Chary, N.S., 2010. Potential for biodegradation and sorption of acetaminophen, caffeine, propranolol and acebutolol in lab-scale aqueous environments. *Journal of Hazardous Materials*, 183, 242-250.

Liu, J.-Z., Song, H.-Y., Weng, L.-P., Ji, L.-N., 2002. Increased thermostability and phenol removal efficiency by chemical modified horseradish peroxidase. *Journal of Molecular Catalysis B: Enzymatic*, 18, 225-232.

Lorphensri, O., Intravijit, J., Sabatini, D.A., Kibbey, T.C.G., Osathaphan, K., Saiwan, C., 2006. Sorption of acetaminophen, 17 α -ethynyl estradiol, nalidixic acid, and norfloxacin to silica, alumina, and a hydrophobic medium. *Water Research*, 40, 1481-1491.

Lu, J., Huang, Q., 2009. Removal of Acetaminophen Using Enzyme-Mediated Oxidative Coupling Processes: II. Cross-Coupling with Natural Organic Matter. *Environmental Science and Technology*, 43, 7068-7073.

Maeng, S.K., Sharma, S.K., Abel, C.D., Magic-Knezev, A., Amy, G.L., 2011. Role of biodegradation in the removal of pharmaceutically active compounds with different bulk organic matter characteristics through managed aquifer recharge: batch and column studies. *Water Research*, 45, 4722-4736.

Mahajan, R., et al., 2010. Comparison and suitability of gel matrix for entrapping higher content of enzymes for commercial applications. *Indian Journal of Pharmaceutical Sciences*, 72, 223-228.

Mazaleuskaya, L.L., Sangkuhl, K., Thorn, C.F., FitzGerald, G.A., Altman, R.B., Klein,

T.E., 2015. PharmGKB summary: pathways of acetaminophen metabolism at the therapeutic versus toxic doses. *Pharmacogenetics and Genomics*, 25, 416-426.

Musson, S.E., Campo, P., Tolaymat, T., Suidan, M., Townsend, T.G., 2010. Assessment of the anaerobic degradation of six active pharmaceutical ingredients. *Science of the Total Environment*, 408, 2068-2074.

National Center for Biotechnology Information. PubChem Compound Database; CID=1983

<https://pubchem.ncbi.nlm.nih.gov/compound/1983> (accessed Nov. 9, 2016).

Nodler, K., Voutsas, D., Licha, T., 2014. Polar organic micropollutants in the coastal environment of different marine systems. *Marine Pollution Bulletin*, 85, 50-59.

Nunes, B., Antunes, S.C., Santos, J., Martins, L., Castro, B.B., 2014a. Toxic potential of paracetamol to freshwater organisms: a headache to environmental regulators? *Ecotoxicology and Environmental Safety*, 107, 178-185.

Nunes, B., Pinto, G., Martins, L., Goncalves, F., Antunes, S.C., 2014b. Biochemical and standard toxic effects of acetaminophen on the macrophyte species *Lemna minor* and *Lemna gibba*. *Environmental Science and Pollution Research*, 21, 10815-10822.

Pal, A., Gin, K.Y., Lin, A.Y. and Reinhard, M., 2010. Impacts of emerging organic contaminants on freshwater resources: review of recent occurrences, sources, fate and effects. *Science of the Total Environment*, 408, 6062-6069.

Parolini, M., Binelli, A., Cogni, D., Provini, A., 2010. Multi-biomarker approach for the evaluation of the cyto-genotoxicity of paracetamol on the zebra mussel (*Dreissena polymorpha*). *Chemosphere* 79, 489-498.

Pedrouzo, M., Reverte, S., Borrull, F., Pocurull, E., Marce, R.M., 2007. Pharmaceutical determination in surface and wastewaters using high-performance liquid chromatography-(electrospray)-mass spectrometry. *Journal of Separation Science*, 30, 297-303.

Petrović, M., Gonzalez, S., Barceló, D., 2003. Analysis and removal of emerging contaminants in wastewater and drinking water. *TrAC Trends in Analytical Chemistry*, 22, 685-696.

Pino, M.R., Val, J., Mainar, A.M., Zuriaga, E., Espanol, C., Langa, E., 2015. Acute toxicological effects on the earthworm *Eisenia fetida* of 18 common pharmaceuticals in artificial soil. *Science of the Total Environment*, 518-519, 225-237.

Proia, L., Osorio, V., Soley, S., Kock-Schulmeyer, M., Perez, S., Barcelo, D., Romani, A.M., Sabater, S., 2013. Effects of pesticides and pharmaceuticals on biofilms in a highly impacted river. *Environmental Pollution*, 178, 220-228.

Rabiet, M., Togola, A., Brissaud, F., Seidel, J.L., Budzinski, H., Elbaz-Poulichet, F., 2006. Consequences of treated water recycling as regards pharmaceuticals and drugs in surface and ground waters of a medium-sized Mediterranean catchment. *Environmental Science and Technology*, 40, 5282-5288.

Radjenović, J., Petrović, M., Barceló, D., 2009. Fate and distribution of pharmaceuticals in wastewater and sewage sludge of the conventional activated sludge (CAS) and advanced membrane bioreactor (MBR) treatment. *Water Research*, 43, 831-841.

Ramos, A.S., Correia, A.T., Antunes, S.C., Gonçalves, F., Nunes, B., 2014. Effect of acetaminophen exposure in *Oncorhynchus mykiss* gills and liver: Detoxification mechanisms, oxidative defence system and peroxidative damage. *Environmental Toxicology and Pharmacology* 37, 1221-1228.

Ranieri, E., Verlicchi, P., Young, T.M., 2011. Paracetamol removal in subsurface flow constructed wetlands. *Hydrology*, 404, 130-135.

Rittmann, B., E., McCarty, P., E., 2001. *Environmental Biotechnology: Principles and Applications*, McGraw-Hill, U.S.A.

Roberts, P.H., Thomas, K.V., 2006. The occurrence of selected pharmaceuticals in

wastewater effluent and surface waters of the lower Tyne catchment. *Science of the Total Environment*, 356, 143-153.

Rodriguez, E.M., Medesani, D.A., Fingerman, M., 2007. Endocrine disruption in crustaceans due to pollutants: a review. *Comparative Biochemistry and Physiology A: Molecular and Integrative Physiology*, 146, 661-671.

Rosal, R., Rodriguez, A., Perdigon-Melon, J.A., Petre, A., Garcia-Calvo, E., Gomez, M.J., Aguera, A., Fernandez-Alba, A.R., 2010. Occurrence of emerging pollutants in urban wastewater and their removal through biological treatment followed by ozonation. *Water Research*, 44, 578-588.

Sakarya, F. K., 2015. Biotransformation of benzalkonium chlorides by immobilized cells of *pseudomonas* sp. biomig1. MSc Thesis, Institute of Environmental Sciences, Boğaziçi University, Turkey.

Santos, L.H., Paiga, P., Araujo, A.N., Pena, A., Delerue-Matos, C., Montenegro, M.C., 2013. Development of a simple analytical method for the simultaneous determination of paracetamol, paracetamol-glucuronide and p-aminophenol in river water. *Journal of Chromatography B: Analytical Technologies in the Biomedical and Life Sciences*, 930, 75-81.

Sarma, S.S., Gonzalez-Perez, B.K., Moreno-Gutierrez, R.M., Nandini, S., 2014. Effect of paracetamol and diclofenac on population growth of *Platyonus patulus* and *Moina macrocopa*. *Journal of Environmental Biology*, 35, 119-126.

Stackelberg, P.E., Furlong, E.T., Meyer, M.T., Zaugg, S.D., Henderson, A.K., Reissman, D.B., 2004. Persistence of pharmaceutical compounds and other organic wastewater contaminants in a conventional drinking-water-treatment plant. *Science of the Total Environment*, 329, 99-113.

Sui, Q., Cao, X., Lu, S., Zhao, W., Qiu, Z., Yu, G., 2015. Occurrence, sources and fate of pharmaceuticals and personal care products in the groundwater: A review. *Emerging*

Contaminants, 1, 14-24.

Ternes, T.A., Stüber, J., Herrmann, N., McDowell, D., Ried, A., Kampmann, M., Teiser, B., 2003. Ozonation: a tool for removal of pharmaceuticals, contrast media and musk fragrances from wastewater? *Water Research*, 37, 1976-1982.

Touahar, I.E., Haroune, L., Ba, S., Bellenger, J.P., Cabana, H., 2014. Characterization of combined cross-linked enzyme aggregates from laccase, versatile peroxidase and glucose oxidase, and their utilization for the elimination of pharmaceuticals. *Science of the Total Environment*, 481, 90-99.

Verlicchi, P., Al Aukidy, M., Zambello, E., 2012. Occurrence of pharmaceutical compounds in urban wastewater: removal, mass load and environmental risk after a secondary treatment--a review. *Science of the Total Environment*, 429, 123-155.

Vulliet, E., Cren-Olive, C., 2011. Screening of pharmaceuticals and hormones at the regional scale, in surface and groundwaters intended to human consumption. *Environmental Pollution*, 159, 2929-2934.

Wu, S., Zhang, L., Chen, J., 2012. Paracetamol in the environment and its degradation by microorganisms. *Applied Microbiology and Biotechnology*, 96, 875-884.

Xu, J.J., Hendriks, B.S., Zhao, J., de Graaf, D., 2008. Multiple effects of acetaminophen and p38 inhibitors: Towards pathway toxicology. *FEBS Letters*, 582, 1276-1282.

Xu, R., Si, Y., Li, F., Zhang, B., 2015. Enzymatic removal of paracetamol from aqueous phase: horseradish peroxidase immobilized on nanofibrous membranes. *Environmental Science and Pollution Research*, 22, 5, 3838-3846.

Yamamoto, H., Nakamura, Y., Moriguchi, S., Nakamura, Y., Honda, Y., Tamura, I., Hirata, Y., Hayashi, A., Sekizawa, J., 2009. Persistence and partitioning of eight selected pharmaceuticals in the aquatic environment: laboratory photolysis, biodegradation, and sorption experiments. *Water Research*, 43, 351-362.

Yu, T.H., Lin, A.Y., Panchangam, S.C., Hong, P.K., Yang, P.Y., Lin, C.F., 2011. Biodegradation and bio-sorption of antibiotics and non-steroidal anti-inflammatory drugs using immobilized cell process. *Chemosphere*, 84, 1216-1222.

Zhang, L., Hu, J., Zhu, R., Zhou, Q., Chen, J., 2013. Degradation of paracetamol by pure bacterial cultures and their microbial consortium. *Applied Microbiology and Biotechnology*, 97, 3687-3698.

Zhou, S., Chan, E., Duan, W., Huang, M., Chen, Y.Z., 2005. Drug bioactivation, covalent binding to target proteins and toxicity relevance. *Drug Metabolism Reviews*, 37, 41-213.

Zion Research; Acetaminophen (Paracetamol) Market for Pharmaceuticals, Dye Industry and Chemical Industry - Global Industry Perspective, Comprehensive Analysis, Size, Share, Growth, Segment, Trends and Forecast, 2014 – 2020.